

CHAPTER – 4

MICROHARDNESS

CHAPTER - IV

Microhardness

I. INTRODUCTION :

Many definitions have been given for hardness from time to time but none has been found proper with enough quantitative interpretation and understanding for the aim and theme. Tuckerman^[1] explained hardness as a hazily conceived aggregate or cogglomeration of properties of a material more or less related to each other. Ashby^[2] defined hardness as a measure of resistance to permanent deformation or damage. The general definition of indentation hardness which is related to the various forms of the indenters, is the ratio of load applied to the surface area of the indentation. Meyer^[3] proposed that hardness should be defined as the ratio of load to the projected area of the indentation. Hence hardness has the dimensions of stress. Thus, the hardness of a solid is defined in general as resistance to deformation. The deformation in turn is a function of interatomic forces^[4]. Mott^[5] and Gilman et al^[6] have shown that the indentation hardness value depends on the crystal structure, nature of bonding and elastic modulus of the crystal and it can be used to determine plastic resistivity against the dislocation motion. .

Chatterjee^[7] further defined indentation hardness as the work done per unit volume of the indentation in a static indentation test for a definite orientation of indenter. On the basis of this definition and Meyer's law,

$P = ad^n$, for spherical indenters, he derived a formula for calculation of hardness. Plendl et al^[8] defined hardness as the pressure or force per square centimeter, which can be conceived as an energy per unit volume and it is in short, the ratio of the input energy and volume of indentation. They further concluded that the resistance itself is a function of the lattice energy per unit volume which is called volumetric lattice energy (U/V), having dimension of ergs/c.c. Here “U” is the total cohesive energy of the lattice per mole and “V” is the molecular volume defined as M/S where “M” is the molecular weight and “S” is the specific heat. Matkin et al^[9] suggested a correlation of hardness with the dislocation theory. They gave a definition of hardness on the basis of generation and movement of dislocations associated with indentation. Later, Westbrook et al^[10] concluded that hardness is not a single properties but it is a rather whole complex of mechanical properties and at the same time a measure of the intrinsic bonding of the material. Gilman^[11] defined hardness as the strength determining parameter which gives information regarding elastic, anelastic, plastic, viscous and fracture properties of both the isotropic and anisotropic solids.

From all these definitions, the basic qualitative meaning of hardness turns out to be a measure of resistance to plastic deformation. Practically, it carries different meanings to different people; for a metallurgist it is resistance to penetration, for a lubrication engineer it is resistance to wear, for a mineralogist it is resistance to scratching, etc.

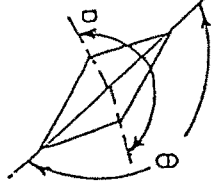
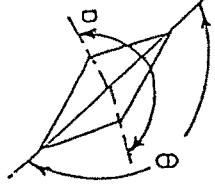
For practical purposes, hardness of the material may be broadly defined as its ability to resist penetration by another particular material. It is a relative property of a material which depends on the elastic and plastic properties of both the penetrated body and the penetrator. In addition to this, hardness of a material depends strongly upon the method of measurement which usually combines in itself various material properties like elastic modulus, yield stress. (which is a measure of plastic behaviour or permanent distortion), physical imperfection, impurities and work hardening capacity. Imperfections created by thermal or mechanical stresses at the time of crystal growth or after it, bear their effect on microscopic properties like electrical resistivity and on macroscopic properties like mechanical strength and in understanding the fracture mechanics, particularly in ductile metals and alloys, etc. In the case of solid solution alloys, to accommodate substitute atoms of greater or smaller size, a change in average interatomic spacing may take place and the solvent lattice may suffer elastic distortion. The distorted lattice causes increased frictional stress to the free movement of dislocations when the alloy is sheared. This means an increase in general hardness.

II. The Static Indentation Hardness Test and Deformation:

The most popular and simplest method of hardness measurement is the static indentation hardness method. Primarily because it does not require

large specimens and on a small specimen a number of measurements can be made. A hard indenter like diamond, sapphire, quartz, steel etc. having specific geometry is applied slowly under load into the surface to be examined and after a certain time of application it is carefully removed from the surface. This results into a permanent indentation mark on the surface. The ratio of applied load to the area of the mark is termed as the hardness of the specimen indented. In this case, the hardness value depends on the geometry of the indenter. If the specimen is anisotropic, the ridging and sinking of material around the mark may produce complicated effects especially with pyramidal indenters (O'Neill)^[12] and it requires correction in the formula used to calculate hardness. To accommodate various shapes, sizes and hardnesses of the specimens, a combination of indenter, load, loading procedure and means of indentation measurements is used. The most commonly used indenters are described in Table-1. Diamond indenters are always used for hard materials in order to minimize errors due to elastic distortion of the indenter. In the case of ball indenters, the hardness number will be independent of load only if the ratio of load to indenter diameter is held constant. For conical and pyramidal indenters, the hardness number will be independent of load for all loads above a certain minimum value depending on specimen material. Knoop indenter with rhomb-based pyramid is used to study the hardness anisotropy of a crystal and to eliminate anisotropy effect, the pentagonal indenter is used (Brookes et al)^[13]. The

TABLE - 1

	Brinell	Rockwell	Vickers	Knoop	Brookes & Mohr
Material of which indenter is made	Hardened steel or tungsten carbide	Diamond	Hardened steel	Diamond	Diamond
Shape of indenter	Sphere	Cone	Sphere	Square based	Rhomb based
Dimensions of indenter	 D = 10MM	 $\theta = 120^\circ$ 1/16 in. 1/8 in. 1/4 in. 1/2 in.	 $\theta = 136^\circ$	 $\theta = 172^\circ - 30'$	 $\alpha = 130^\circ$ $\theta = 172^\circ - 30'$
Characteristics	1. Geometrically similar impressions are not obtained	1. Prepares the surface upon which the further penetration due to major load is based 2. Hardness is read directly on the dial gauge 3. Hardness value may be appreciable in error due to large amount of recovery along depth	1. Geometrically similar impressions are obtained	1. Hardness of upper most surface layer can be found 2. Sensitive to anisotropy of crystals. 3. Shorter diagonal undergoes recovery	1. Eliminates the anisotropy normally observed in hardness with all other indenters.

description of various indenters shows that the method of indentation can easily be applied to all kinds of crystalline materials under their own suitable conditions of temperature and environment. Though the static indentation method is very simple, it results in a complex development of the stress fields especially in the crystalline materials.

Indenters have been known to be either sharp or blunt according as their included angles are less or greater than 90°. As this angle increases, the indenter tends to be blunt and the influence of friction and prior strain hardening decreases. Also the value of constraint factor C in the relation between hardness and yield stress, i.e., $H = CY$, tends to 3 as the effective cone angle increases^[14]. The stress field produced by such an indenter closely approximates to the prediction of elastic theory. The Vickers diamond pyramidal indenter used in the present study has the included angle of 136° which is a good compromise to minimize frictional effects and at the same time to give a well defined geometrical square shape to the indentation mark. Also for metal to diamond contact, the coefficient of friction ranges from about 0.1 to 0.15 making the frictional effects less pronounced^[14]. The Vickers hardness is defined as the ratio of applied load to the pyramidal contact area of indentation and turns out to be

$$H_v = \frac{1854 \times P}{d^2} \times 9.8 \text{ MPa} \quad \dots\dots 1$$

where, H_v = Vickers hardness
 d = mean diagonal of the indentation mark in μm
 p = applied load in gm.

Single crystals are known to deform by the process of slip, deformation twinning, crack and fracture. Slip is displacement of one part of crystal relative to another along certain definite crystallographic planes and directions. Usually the slip planes and directions are of low indices and of close packing.

Deformation in some crystals is dominated by twinning. In this case, a crystal changes the lattice orientation at deformation site, with respect to the undeformed matrix. Twinning is simple sliding of one plane of atoms over another plane and the movement of each plane is proportional to its distance from the twinning plane^[16]. In the study of microhardness anisotropy of zinc and manganese single crystals, Partridge et al^[17] observed deformation twins and the resolved shear stress criterion usually applicable to the slip mechanism was found insufficient to account for the observed distribution of twins. Any analysis which attempts to relate deformation twinning with hardness anisotropy must take into account the dimensional changes which occur during twin deformation. The slip and twinning of diamond were reported by Phaul^[18] with a diamond indenter indenting on the flat and smooth surface of diamond. Similar results were observed in the case of molybdenum carbide single crystals using Knoop and Vickers indenters^[19].

Tolansky et al^[20] studied the Vickers indented surface of steel, tin and bismuth and using interferometry, observed maximum distortion along the medians bisecting the sides of the square mark and minimum along the diagonals. They finally concluded that the symmetry in the fringe pattern is purely crystallographic and it has nothing to do with the orientation of the square of the indentation mark. They also concluded that in the interference pattern, the convex sides corresponding to extended wings were “piled-up” regions and concave sides were “sunked-in” regions. Though plastic deformation is known classically as the permanent deformation left in a body after removal of load or deformation stress, the present day trend defines plastic deformation as the deformation in which creation or motion of dislocations is involved. The phenomena of crack and fracture are classified as ductile or brittle according as whether or not they involve plastic deformation in their nucleation and propagation. In addition to these, there are other deformation modes, but unlike deformation twinning, these phenomena occur in an irregular way producing inhomogeneous deformation. However, these are not considered as independent mechanisms. Irrational twins, kink bands, deformation bands, Brillantov-Obreimov bands etc. are of this type. Crocker and Abell^[21] have pointed out that the phenomenon known as kinking and for a long time known to be governed by slip processes in Zn^[22] and in Ni^[23], can be considered as a deformation mechanism in its own right. The occurrence and amount of deformation produced by different

mechanisms depend on various factors such as crystal structure, nature of atomic bonds, strain rate, temperature, impurities, method of deformation, crystallographic orientation of the deformation stress axis with respect to the crystal, etc. The general aspects of deformation by slip and twinning have been treated by various authors^[24-27]. The basic theory of crack and fracture has been reviewed extensively and treated in various reports^[28-29].

III. Microhardness of Bi₂Te₃: Sb,Sn,Se Single Crystals

Applied load Dependence :

From the geometrically similar shapes of the indentation marks for various loads, it can be shown that the hardness is independent of load, though it is not true experimentally for certain ranges of applied load. The hardness obtained by the indentation tests is not the actual hardness prior to indentation. This is so because the indentation process deforms the indented region of the sample. This deformation has to bear its effect in responding to the progressive penetration of the indenter. Usually at low applied loads, the deformation causes work hardening of the surface layers. Hence, the measured hardness is more than the actual. The main findings in this respect are briefly given below.

The variation of hardness with load was explained in terms of slip in Te crystals^[30]. Knoop^[31] and Bernhardt^[32] observed increase in hardness with

decrease in load. Campbell et al^[33] and Mott et al^[34] observed decrease in hardness with decrease in load. Taylor^[35] and Bergsman^[36] observed no significant change in hardness by varying load. A relationship between microhardness and applied load has been given by Meyer^[37] as $P = ad^n$ where P = applied load, d = diagonal of the indentation mark and a and n are constants. In the case of Vickers microhardness, the value of the exponent n is equal to 2 for all indentation marks. It implies a constant hardness value for all loads. Hanemann^[38] concluded that in the low load region, n has a value less than 2. While Onitsch^[39] found the value of n between 1 and 2. Grodzinski^[40] found variation of n from 1.3 to 4.9. However, most of the values of n were found to be 1.8. Though hardness would be expected to be constant, the actual results obtained by different workers, revealed disparities amounting to 30 to 50%. Due to this variation, a high load region has to be selected which leads to the definition of a load independent value of microhardness. The scattered results may be attributed to the following reasons :

- 1) Meyer's law ($P = a \times d^n$) is not valid
- 2) Microstructures exercise a considerable influence on measurements involving very small indentations.
- 3) Experimental errors due to mechanical polishing, penetration of specimen, vibration, loading rate, shape of indenter and measurement of impression affect the hardness value considerably.

Though the range of macro and micro indentations are not principally defineable, in practice, two possible regions can usually be recognized :

(1) Microhardness :-

From the lowest possible loads up to a maximum, which may be around 50 gms.

(2) Macro or Standard hardness :-

For loads over a high value, which may be around 500 gm or more.

In the works reported by many workers from 1960 onwards, hardness has been found to vary with load at low loads and under higher loads it has been found to be constant.

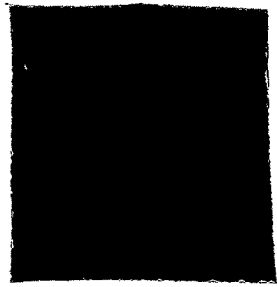
The Vickers diamond pyramidal indenter was used for the microhardness indentation tests on the cleavage planes (111) of the $\text{Sb}_{0.2} \text{Bi}_{1.8} \text{Te}_3$, $\text{Sn}_{0.2} \text{Bi}_{1.8} \text{Te}_3$ and $\text{Bi}_2\text{Te}_{2.8} \text{Se}_{0.2}$ crystals. The crystals used for the indentation tests were all obtained by the Bridgman method at the speed of 4mm/hr. The cleavage slices of thickness about 2 to 3mm were obtained by cleaving the crystal at 0°C. Indentation tests under selected parameters were repeated at least three times and the average results are taken into account.

To decide the loading time to be kept constant for the hardness tests at room temperature, experiments were performed for various loading times from 5 sec to 60 sec, keeping applied load constant at 490 mN which is a sufficiently high load for which the hardness was observed to be insensitive

to small load variations.

The indentation time in the hardness test is an important parameter, particularly for those materials which exhibit creep characteristics at ordinary temperatures. When studying dependence of hardness on load, orientation and temperature, the loading time should be kept constant. To determine the loading time to be kept constant one should examine the time dependence of hardness.

The hardness decreases with loading time and does not saturate even up to a loading time as high as 60 sec. The hardness value at around 50 to 60 sec corresponds to the indentation mark nearly the size of the field of view of micrometer eyepiece. Therefore a compromise was made and a time of 20 sec was chosen, this also being a recommended loading time by the manufacturers of the hardness tester. Therefore for studying hardness variation with load, temperature and orientation, 20 sec was selected as the constant loading time. The indentations were performed at a very slow rate and for all indentations care was taken to see that the rate was nearly the same. Also, between two neighbouring indentation marks on the same surface, a separation of at least two indentations was maintained to avoid interference. The indentation mark produced was square in shape (Figure-1). The diagonals of indentation mark were measured using micrometer eyepiece. The least count of the eyepiece was 0.19 micron.



X1900

Fig. 1

Vickers hardness tests were carried out under different applied loads from 9.81mN to 981mN at room temperature (303K). Figure 2 shows the plot of Vickers hardness H_v v/s load P in the case of $Sb_{0.2}Bi_{1.8}Te_3$ single crystals. Figures 3 and 4 show similar plots obtained, respectively, for the $Sn_{0.2}Bi_{1.8}Te_3$, and $Bi_2Te_{2.8}Se_{0.2}$ single crystals. The plots indicate clearly that there is a complex dependence of H_v on load, particularly for loads less than 200mN. In this low load range (LLR), the hardness exhibits an initial increase with load followed by a maximum. This maximum occurs around 50mN for all the crystals. With further increase of load the hardness decreases and saturates at about 250 to 300mN.

In respect of the above results, it should be noted that the hardness is known to vary considerably in the low load range because the work hardening capacity and elastic recovery of a particular material are dependent on the load, the nature of surface indented and the depth to which the surface is penetrated by the indenter. For example, the low load hardness behaviour in the case of silicon single crystal has been explained on the basis of elastic recovery and piling up of material around the indentation mark^[41]. Both the magnitude of work hardening and the depth to which it occurs are the greatest for the soft metallic materials which can be appreciably work hardened. Since the penetration depth at high loads is usually greater than that of the work hardened surface layer, the hardness value at high loads will be representative of the undeformed bulk of the material and hence the Vickers hardnesses of

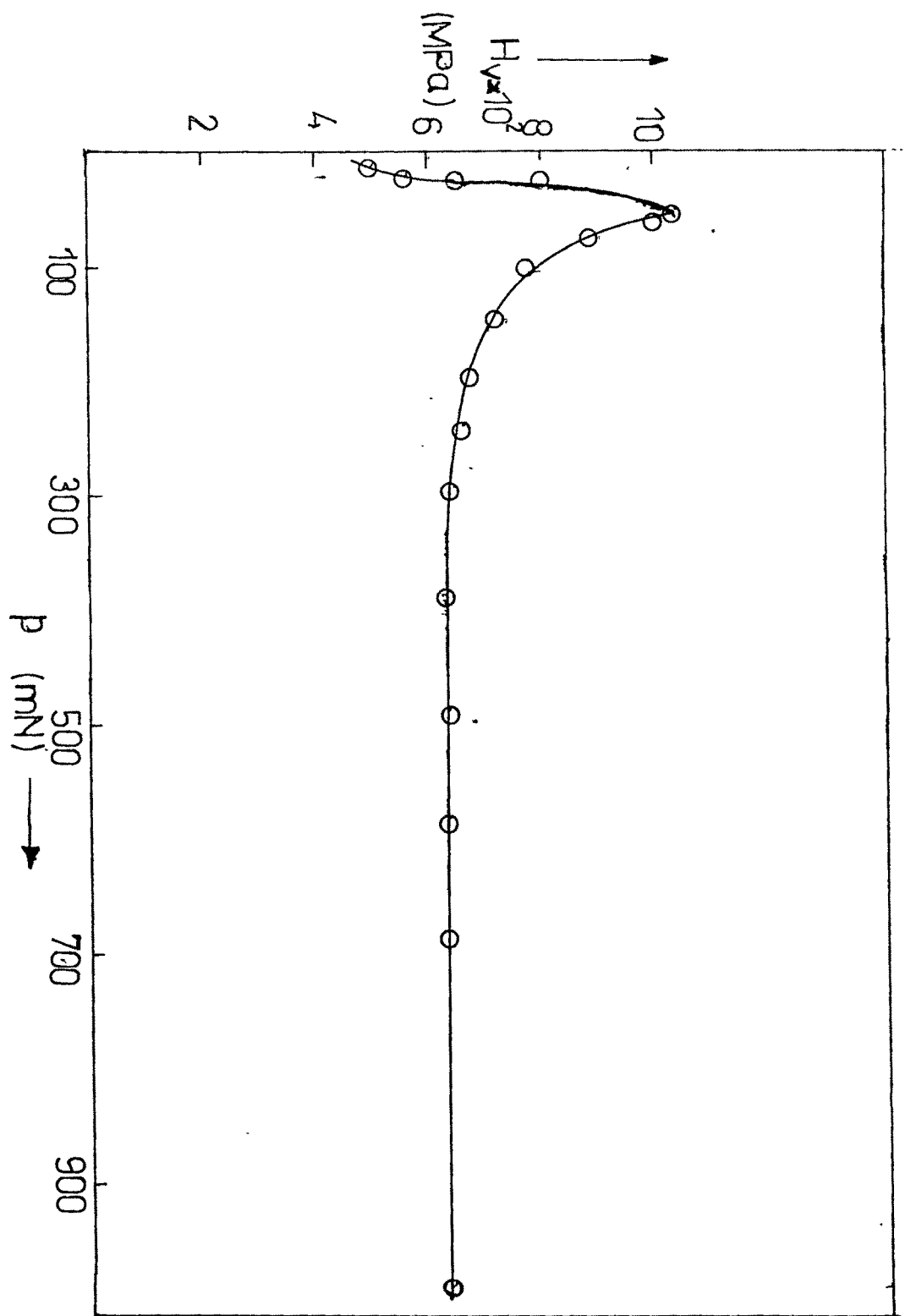


Fig. 2

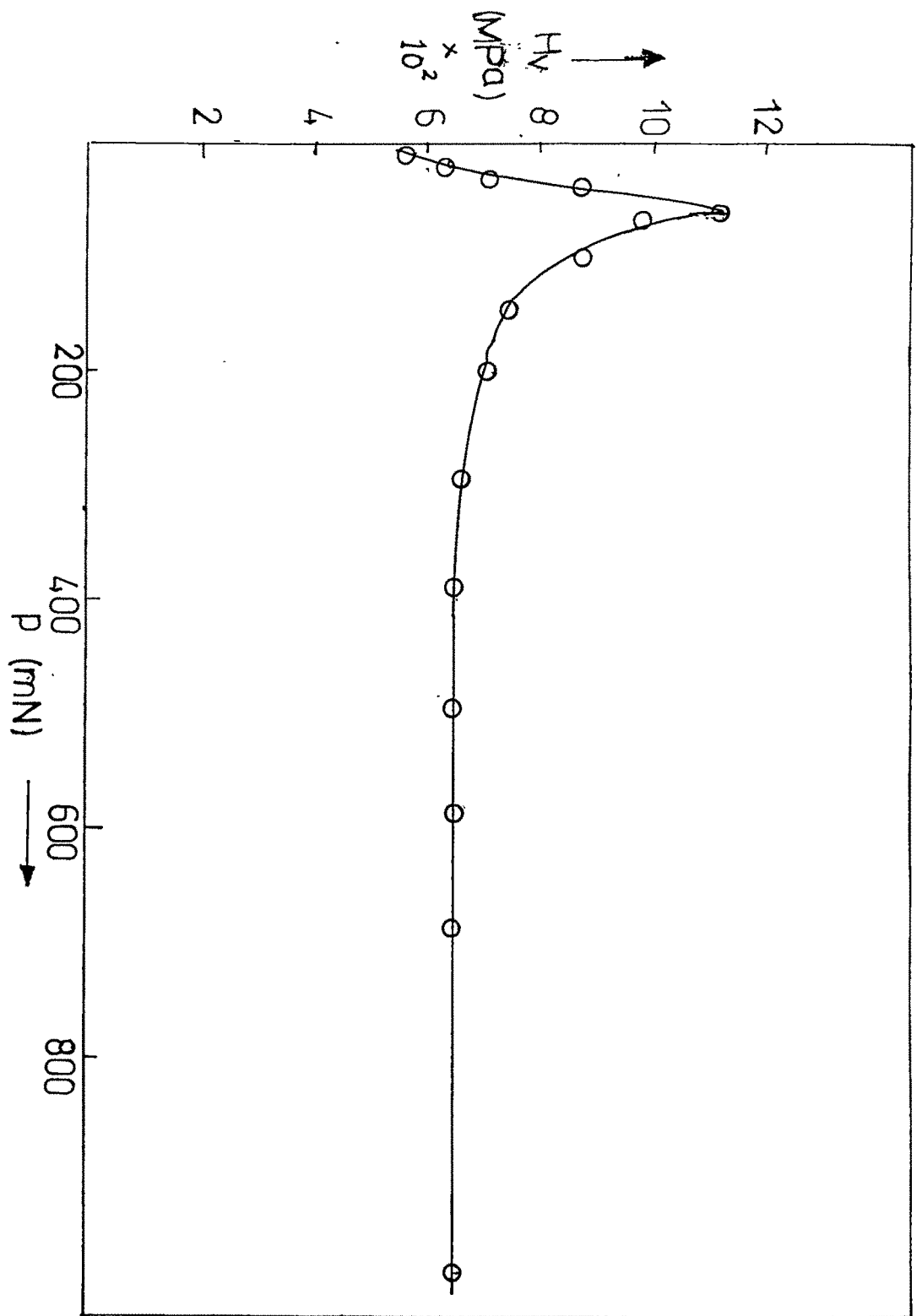


Fig. 3

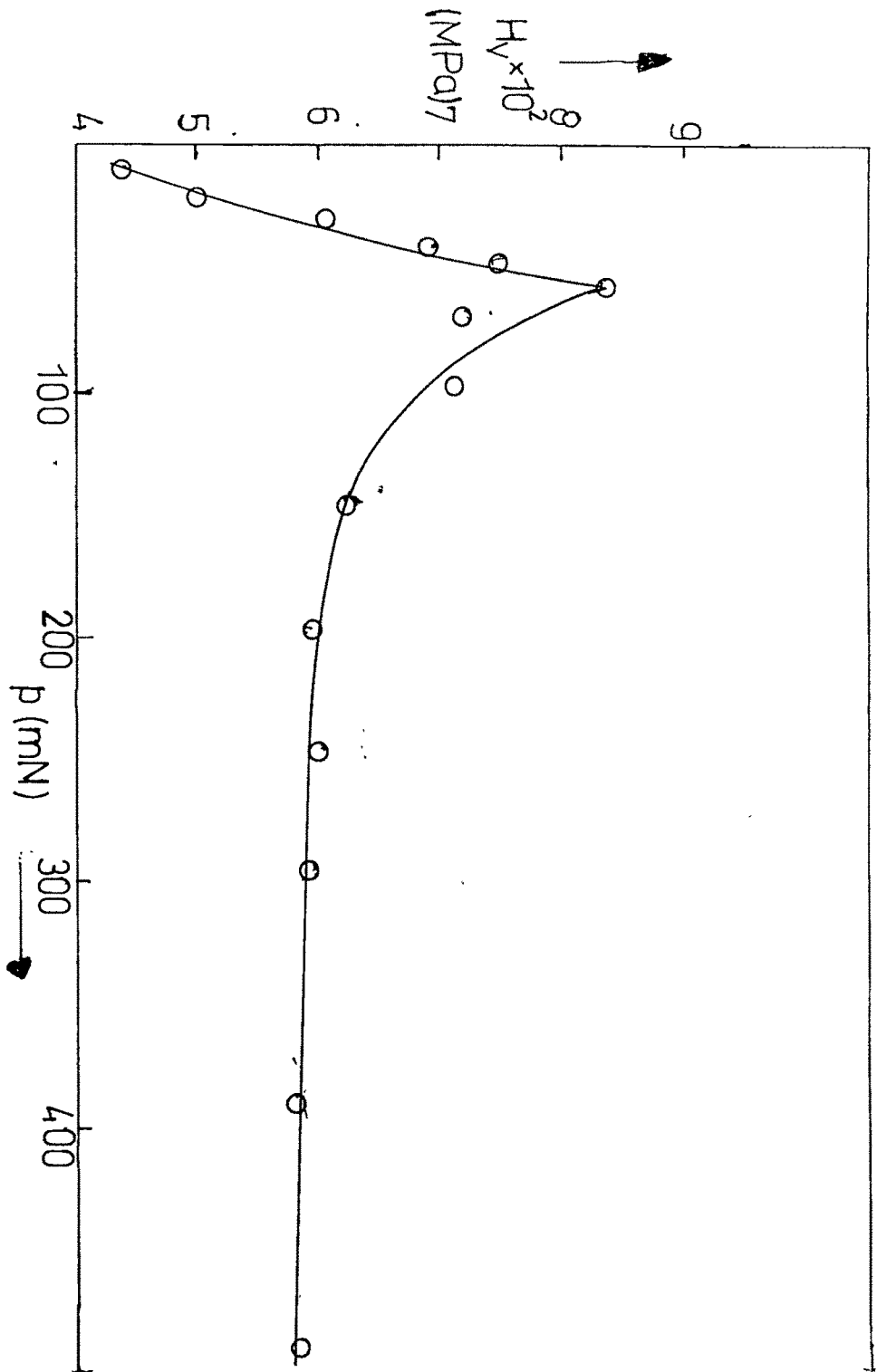


Fig. 4

$\text{Sb}_{0.2}\text{Bi}_{1.8}\text{Te}_3$, $\text{Sn}_{0.2}\text{Bi}_{1.8}\text{Te}_3$, and $\text{Bi}_2\text{Te}_{2.8}\text{Se}_{0.2}$ single crystals are 630 Mpa, 642 Mpa and 582 Mpa, respectively, as can be seen from the plots.

As has been pointed out, the nature of H_v v/s P plot in the LLR is characteristic of the phenomena occurring in the surface layers penetrated by the indenter. Now the depth of penetration depends usually on three factors :

1) The type of surface receiving the load which can again be divided into three categories :-

- a) Surface layer having different degree of cold working^[42]
- b) Surface layer having finely precipitated particles^[43] and
- c) Surface layer having different grain size^[44] and number of grains indented^[45], if the specimen is a polycrystal.

2) The magnitude of the applied load and

3) Accuracy in the normal operation of indenting the specimen and the rate at which the indentation is carried out, i.e. the strain rate. The time taken to realize the full load will evidently decide the strain rate.

All these factors play a prominent role when hardness tests are carried out by indentation at low loads. The surface layer-sensitive initial increase in hardness with load can be explained in terms of strain hardening based on dislocation theory. It is known that dislocations are surrounded by elastic stress fields. The stress fields of different dislocations interact strongly and lock the dislocations into metastable configurations. The effect becomes quite pronounced in metals where the dislocation mobility is usually high.

Individual dislocations move readily at much lower stresses. The flow that occurs during indentation is therefore not limited by drag on isolated dislocations. The interactions between dislocations create jogs on them and these jogs create trails of dislocation dipoles behind the moving dislocations. As the penetration proceeds, the structure soon becomes filled with interacting dislocations forming complex networks resulting into efficient barriers to the motion of new dislocations. Further flow is then limited by the strength of interaction between the barriers and dislocations. The externally applied stress required to produce further plastic deformation must be sufficient to make the dislocation move through the opposing stress fields of these interactions. The effective dislocation zones in the damaged layer causing such back stresses may correspond to what are known as “coherent regions”^[46-47].

The load dependence of hardness in LLR (Figure-2 ,3 and 4) may be plausibly explained in terms of coherent regions. The presence of coherent regions has also been evidenced clearly by the depth profile of dislocation etch pit distributions below the indentations in the case of silver single crystals^[48]. The coherent regions in the present case accordingly extend to the depth of penetration of the indenter under the loads corresponding to the hardness peaks. Thus the increase in hardness with load in the low load range gets limited by the extent of the coherent region.

The constant, characterizing the load dependence of hardness, that is

the Meyer index n was obtained by plotting $\ln P$ versus $\ln d$. These plots are shown in Figures 5,6 and 7,. It can be seen that these plots exhibit two linear regions in correspondence with the respective H_v versus p plots in Figures 2,3 and 4. Accordingly, the two slopes, i.e. the Meyer index values n_1 & n_2 , are listed in Table-2. The n_1 values are seen to be significantly greater than 2. This reflects the fact that the hardness is strongly dependent on load in the LLR. This dependence is maximum for $\text{Sn}_{0.2}\text{Bi}_{1.8}\text{Te}_3$ ($n_2 = 4.82$) implying high rate of increase of hardness with load in LLR. Thus among the three crystal, $\text{Sn}_{0.2}\text{Bi}_{1.8}\text{Te}_3$ has been observed to possess the maximum work-hardening capacity. The n_2 values are closer to the ideal value 2 indicating that the hardness tends to become independent of the applied load at sufficiently high loads, a fact also observed in Figures 2,3 and 4.

Indentation Hardness Creep:

This part reports the results obtained in the study of variation of microhardness with time at different temperatures of single crystals of $\text{Sb}_{0.2}\text{Bi}_{1.8}\text{Te}_3$, $\text{Sn}_{0.2}\text{Bi}_{1.8}\text{Te}_3$ and $\text{Bi}_2\text{Te}_{2.8}\text{Se}_{0.2}$. The Vickers microhardness indentation tests were carried out on the cleavage surfaces of the crystals using a constant load and varying the time of indentation. The tests were repeated at different temperatures. The results obtained have been used to determine the activation energy for creep.

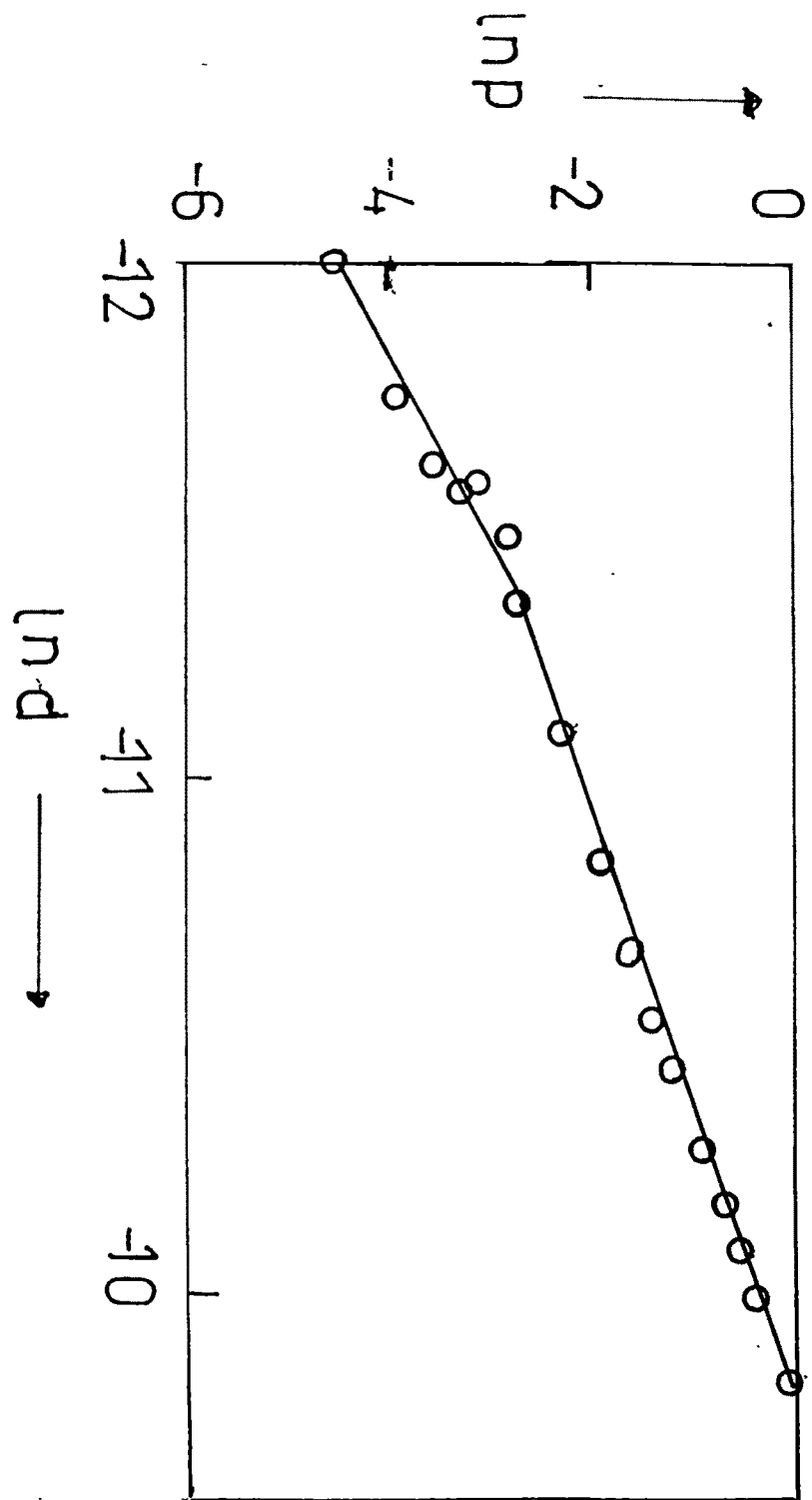


Fig. 5

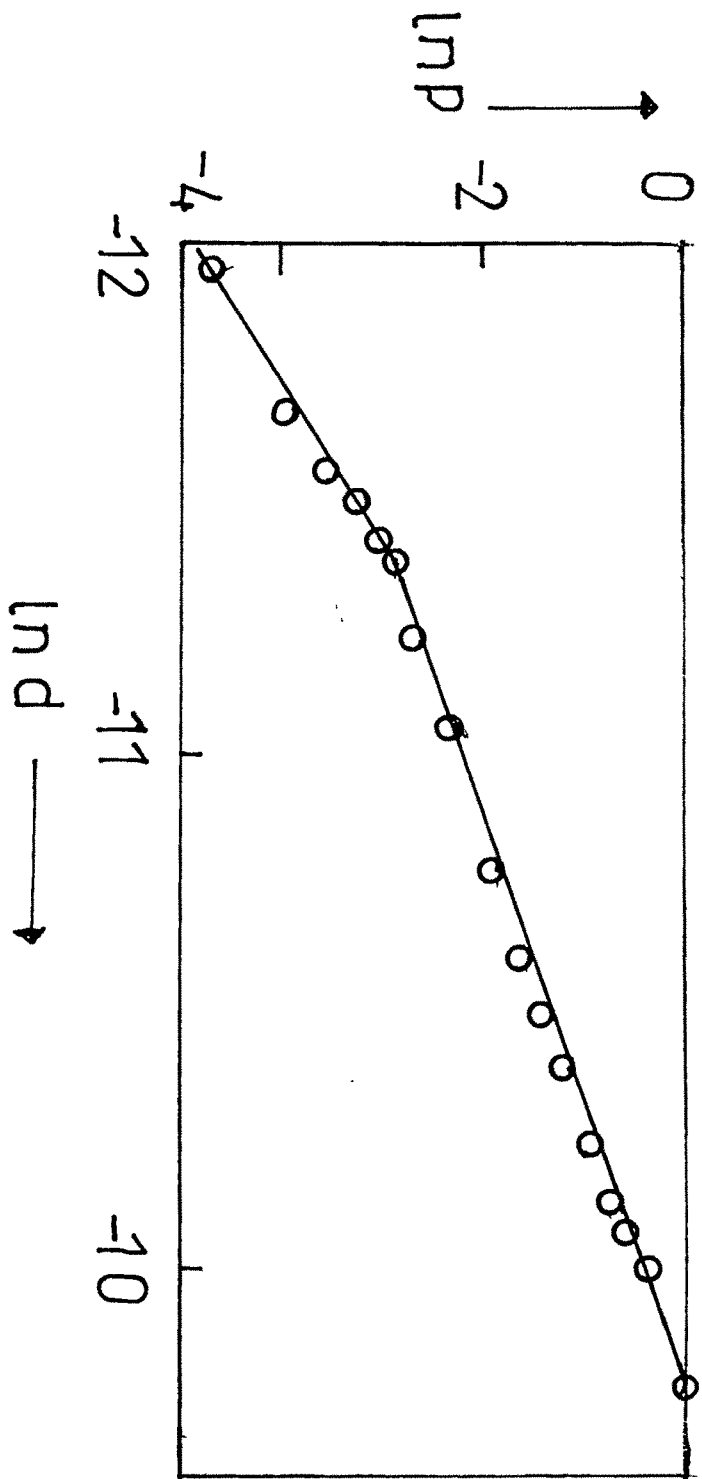


Fig. 6

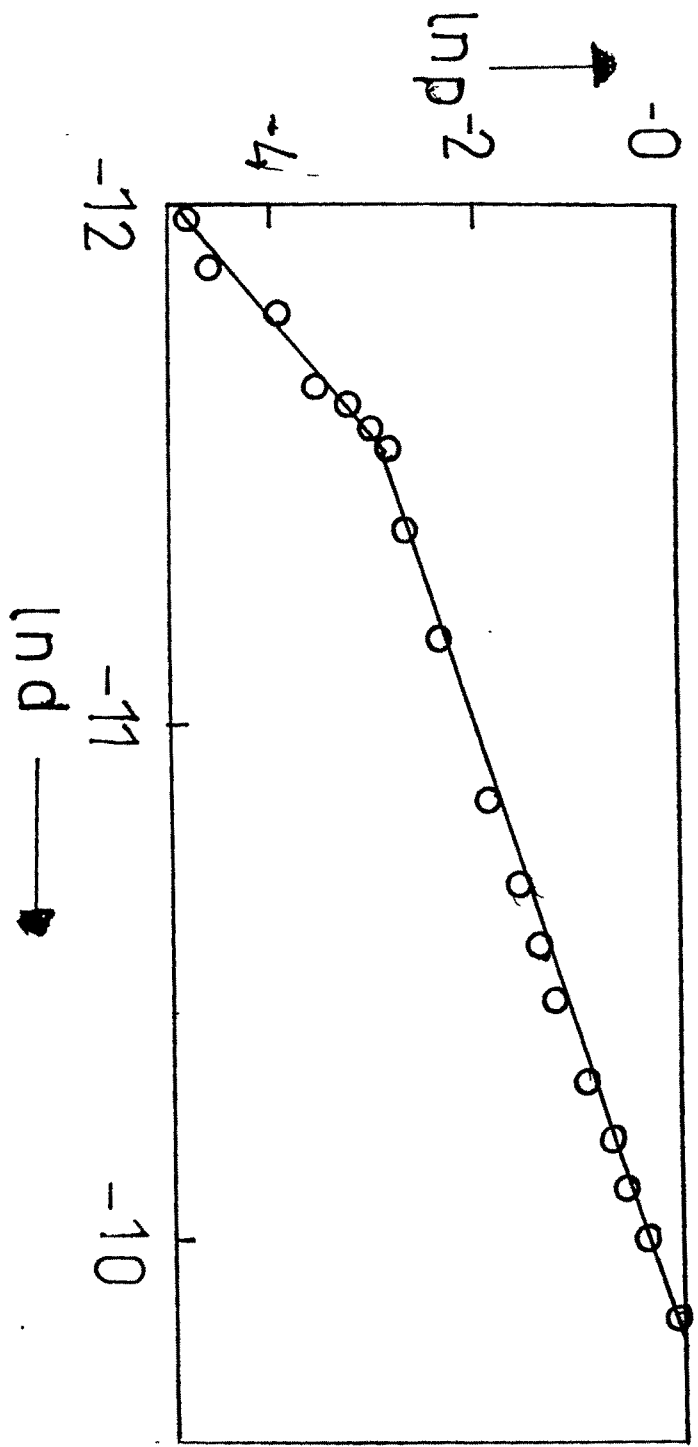


Fig. 7

Table-2

Crystals	Meyer Index	
	n_1	n_2
$\text{Sb}_{0.2}\text{Bi}_{1.8}\text{Te}_3$	2.83	1.79
$\text{Sn}_{0.2}\text{Bi}_{1.8}\text{Te}_3$	4.82	1.79
$\text{Bi}_2\text{Te}_{2.8}\text{Se}_{0.2}$	3.28	1.71

In assessing the strength of a crystal the indentation method assumes the hardness of a crystal to be independent of time after the load is fully applied. In fact, the indenter generally sinks into the crystal surface even after the application of full load. This is known as indentation creep. The use of indentation hardness is well known for the study of plastic yield properties of solids. The general behaviour regarding the decrease in the hardness with increasing loading time may be described by an empirical formula which incorporates the earlier relations given by the previous workers ^[49-51]. The behaviour of hardness closely parallels the creep characteristics of materials in unidirectional stress tests. Using a transient creep equation derived by Mott^[52] for constant stress conditions and assuming that it can be applied even when the stress changes, Atkins et al^[53] analyzed the kinematics of creep process during indentation. They obtained good agreement between theory and experiment. Activation energy derived from the hardness measurements were close to the activation energies for self-diffusion. Their analysis suggested that in spite of its limited validity, a transient creep equation of state may be used to describe the hardness behaviour of solids at elevated temperatures. The nature and amount of creep characteristics depend on temperature.

The time-dependence of microhardness was studied in this laboratory on different single crystals by various workers (Jani T. M., Shah R.T., Desai C.F., Shah A. J., Shah R. C. and Vyas S. M.) ^[54-59]

For the analysis of the data, the well established relation given by Atkins et al^[53] is used. The relation is as under.

$$H^{-3} - H_0^{-3} = A \exp(-Q/3RT) (t^{1/3} - t_0^{1/3}) \quad \text{-----2}$$

where,

H = the hardness value at time t_0 ,

H_0 = the hardness value immediately after attaining the full load P
at time t_0 .

t = time

Q = Activation energy for creep

R = the gas constant

A = constant

T = absolute temperature

The equation can be written in a convenient form as

$$\ln(H^{-3} - H_0^{-3}) = \ln a + \ln(t^{1/3} - t_0^{1/3}) - Q/3RT \quad \text{-----3}$$

All the observations were obtained on freshly cleaved (111) faces of these crystals, using Vickers pyramidal indenter. A constant load of 492mN was used, for which the hardnesses of $Sb_{0.2} Bi_{1.8} Te_3$, $Sn_{0.2} Bi_{1.8} Te_3$ and $Bi_2 Te_{2.8} Se_{0.2}$ crystals were found to be virtually independent of load. The

indentations of the specimens were carried out at 303K, 323K, 353K, 373K and the indentation time was varied from 5 sec to 60 sec at each temperature. The temperature could not be exceeded beyond 373K since there is no provision of heat-shield on the hardness tester used to prevent possible damage of indenter-objective at high temperature.

It has been observed that when all other parameters are kept constant, the microhardness decreases with increasing temperature. Shishokin-Ito^[49-50] has given the relation

$$H_v = A \exp (-BT) \quad \text{-----4}$$

where the constant B is known as softening parameter and A, the extrapolated intrinsic hardness.

Figures-8,9 and 10 show the plots of $\ln H_v$ v/s T / T_m obtained respectively for $Sb_{0.2} Bi_{1.8} Te_3$, $Sn_{0.2} Bi_{1.8} Te_3$ and $Bi_2 Te_{2.8} Se_{0.2}$ crystals. In all these cases the indentation time was 20 sec. In the above graphs, T_m is the melting point of the crystal. The plots are seen to obey the above relation. From graphs, the softening parameters of $Sb_{0.2} Bi_{1.8} Te_3$, $Sn_{0.2} Bi_{1.8} Te_3$ and $Bi_2 Te_{2.8} Se_{0.2}$ crystals were found to be $132.40 \times 10^{-4} K$, $162.60 \times 10^{-4} K$ and $84.5 \times 10^{-4} K$, respectively. Similar decrease in hardness with temperature was found in the cases of Si, Ge and Cu crystals^[10,14,47].

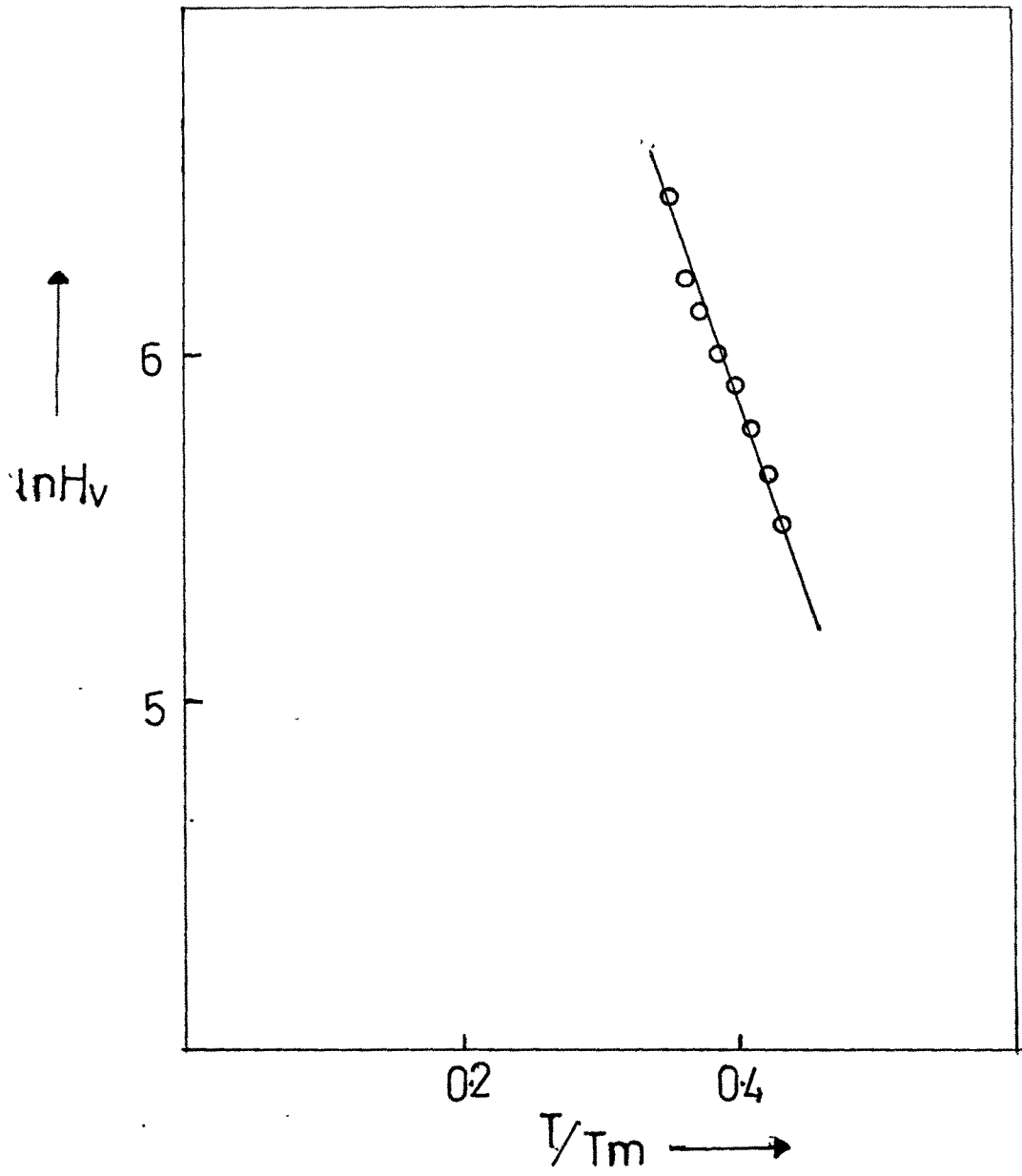


Fig. 8

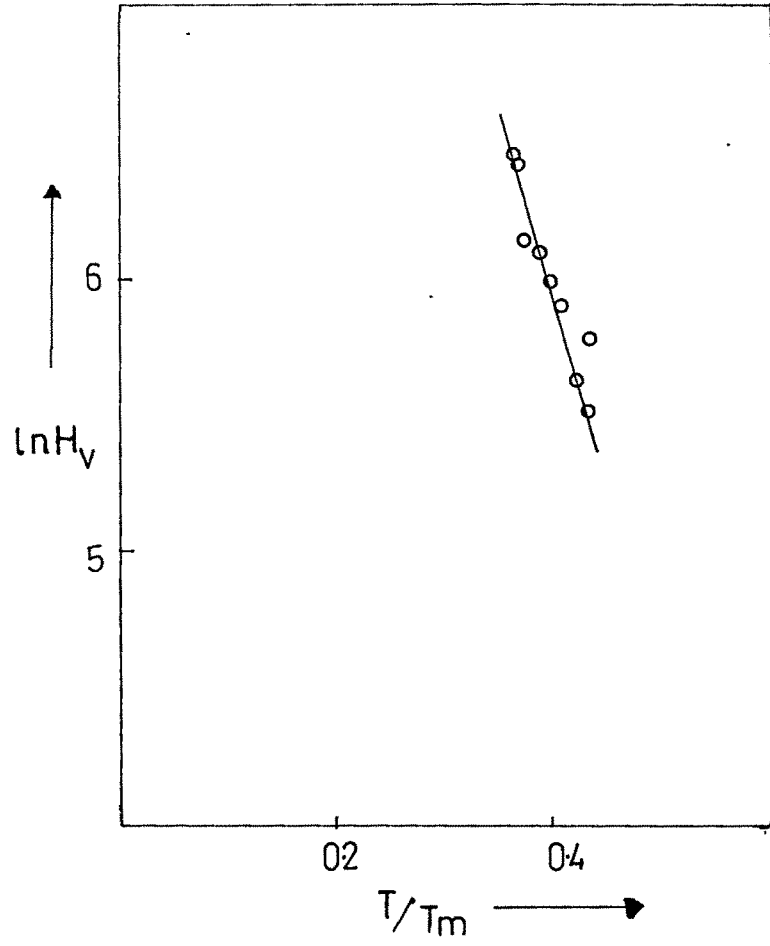


Fig. 9

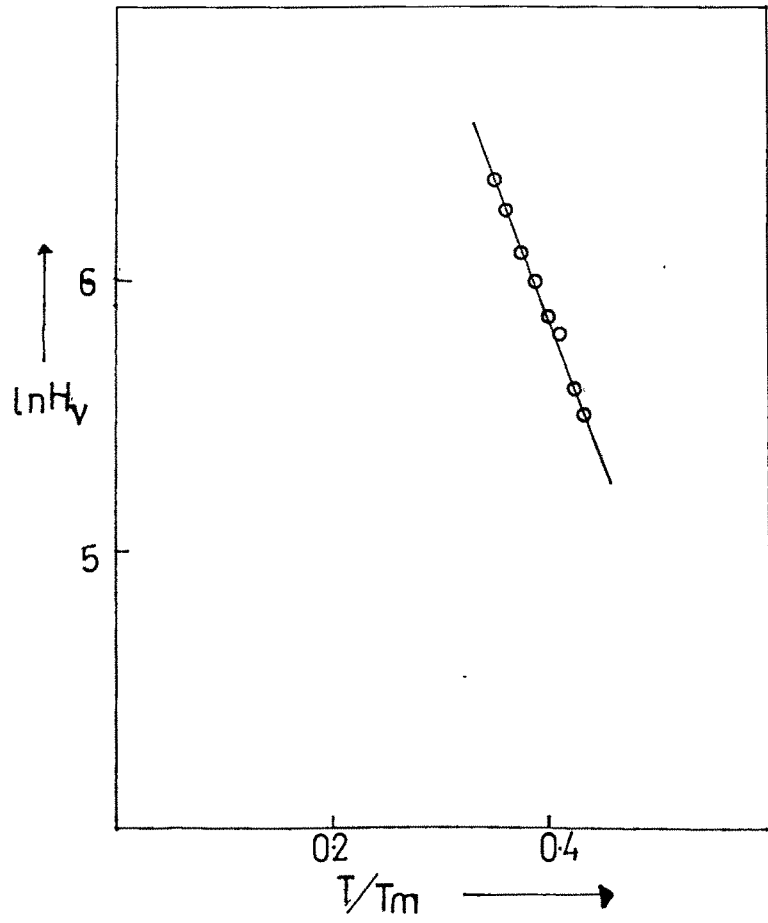


Fig. 10

The experimental observation needed to calculate Q are shown in the form of $\ln H_v$ v/s $\ln t$ plots in Figures-11,12 and 13 respectively for $Sb_{0.2} Bi_{1.8} Te_3$, $Sn_{0.2} Bi_{1.8} Te_3$ and $Bi_2 Te_{2.8} Se_{0.2}$ crystals. These are straight lines obtained at the temperatures indicated near each graph. From the nature of the graphs it is clear that the $\ln H_v$ varies linearly with $\ln t$. It has been predicted by Atkins et al^[53] that the negative slope of such straight lines should increase with increasing temperature. However, the present author is unable to draw any such conclusion, due to limited range of temperatures used.

The value of H_0 at time t_0 , selected as one second, was obtained by extrapolating the straight lines to $\ln t = 0$ and the intercepts on $\ln H_v$ axis give the values of H_0 for different temperatures. Using these values of H_0 and t_0 , $\ln(H^3 - H_0^{-3})$ and $\ln(t^{1/3} - t_0^{1/3})$ were calculated and also plotted as shown in Figures 14,15 and 16, respectively, for $Sb_{0.2} Bi_{1.8} Te_3$, $Sn_{0.2} Bi_{1.8} Te_3$ and $Bi_2 Te_{2.8} Se_{0.2}$ crystals. The straight lines have nearly equal slopes close to unity as predicted by equation (2). The value of activation energy, Q, for creep was calculated by finding the difference between the intercepts at two temperatures T_1 and T_2 in these graphs and equating them to

$$\frac{Q}{3R} (1/T_2 - 1/T_1) \text{ -----} 5$$

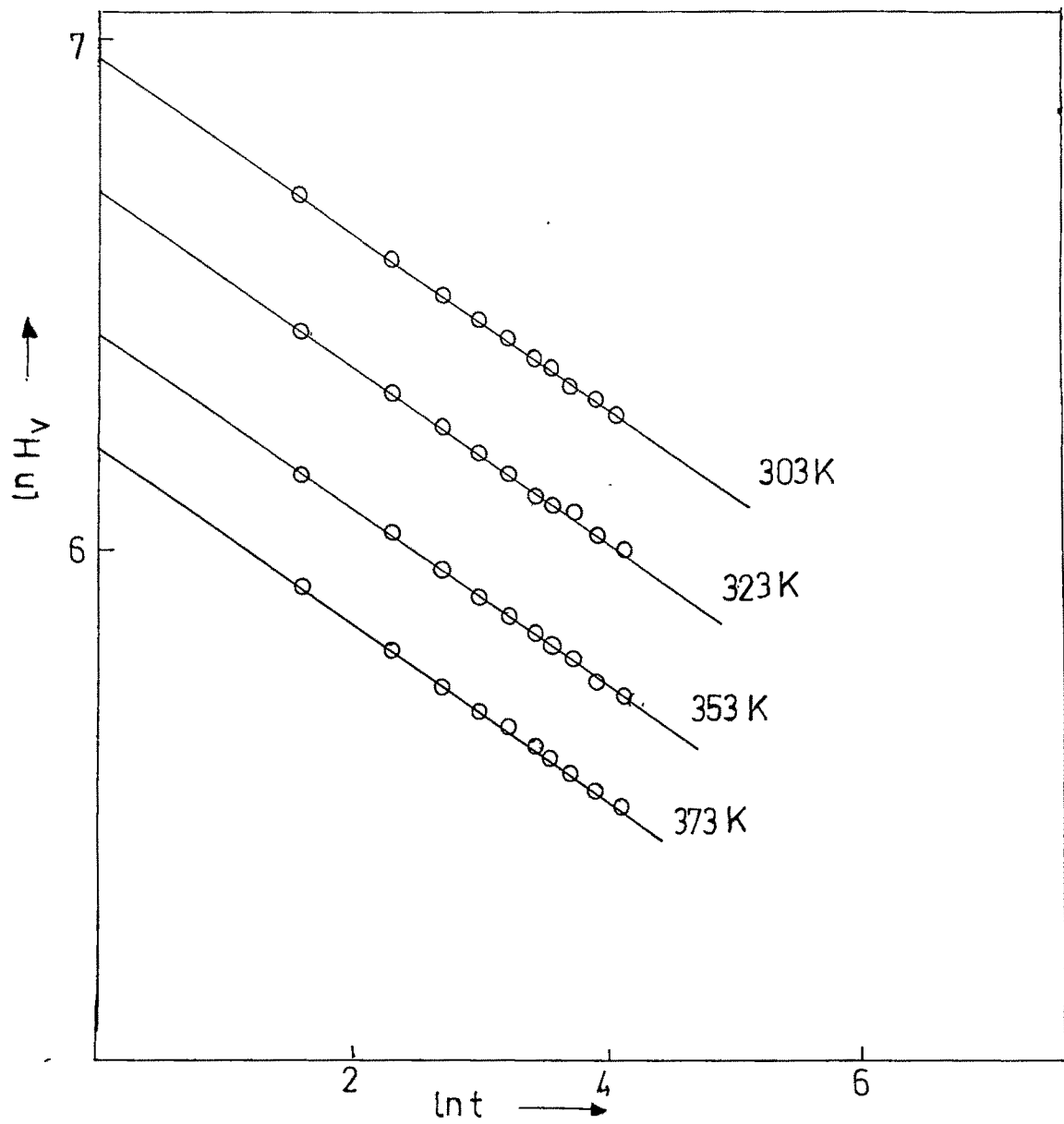


Fig. 11

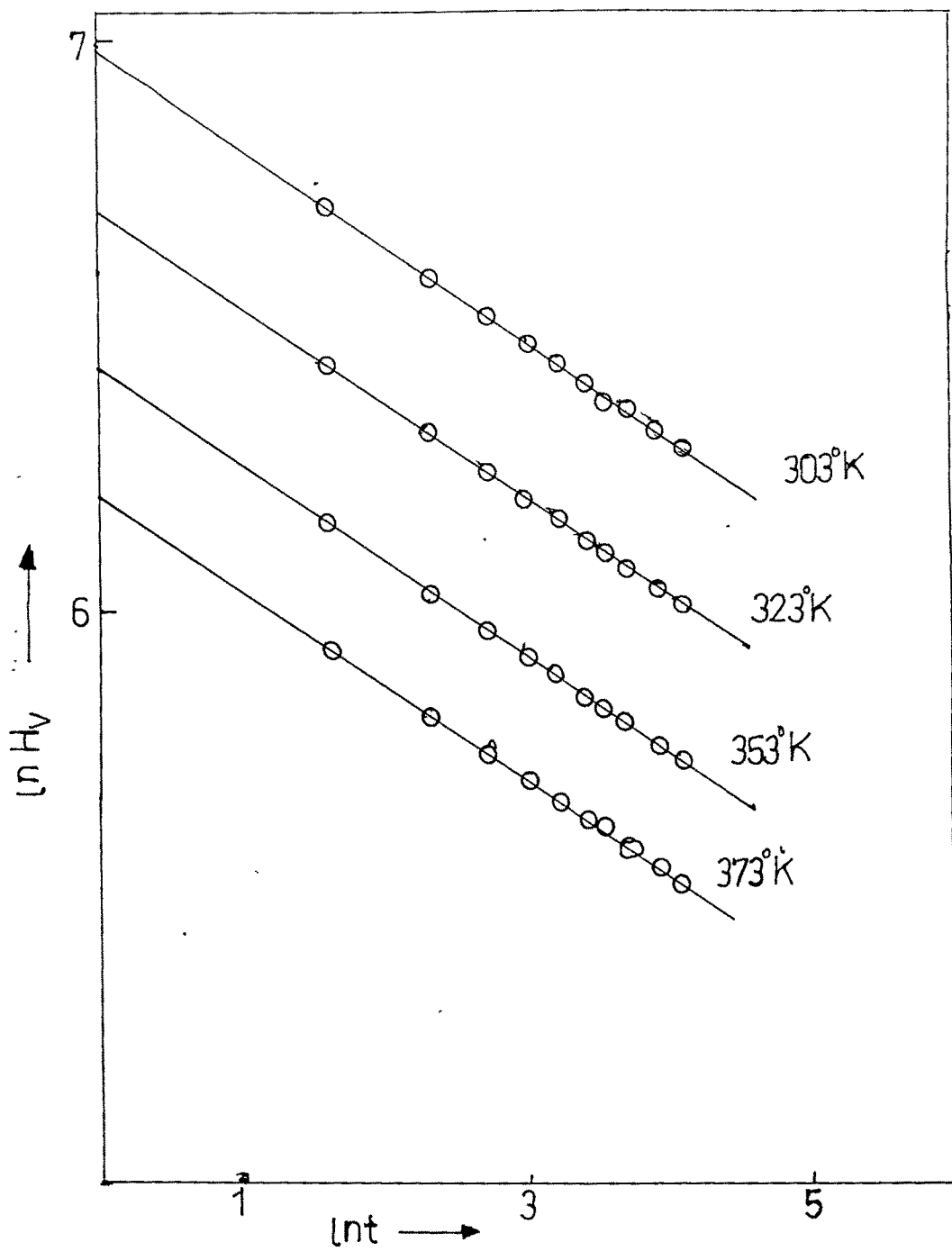


Fig.12

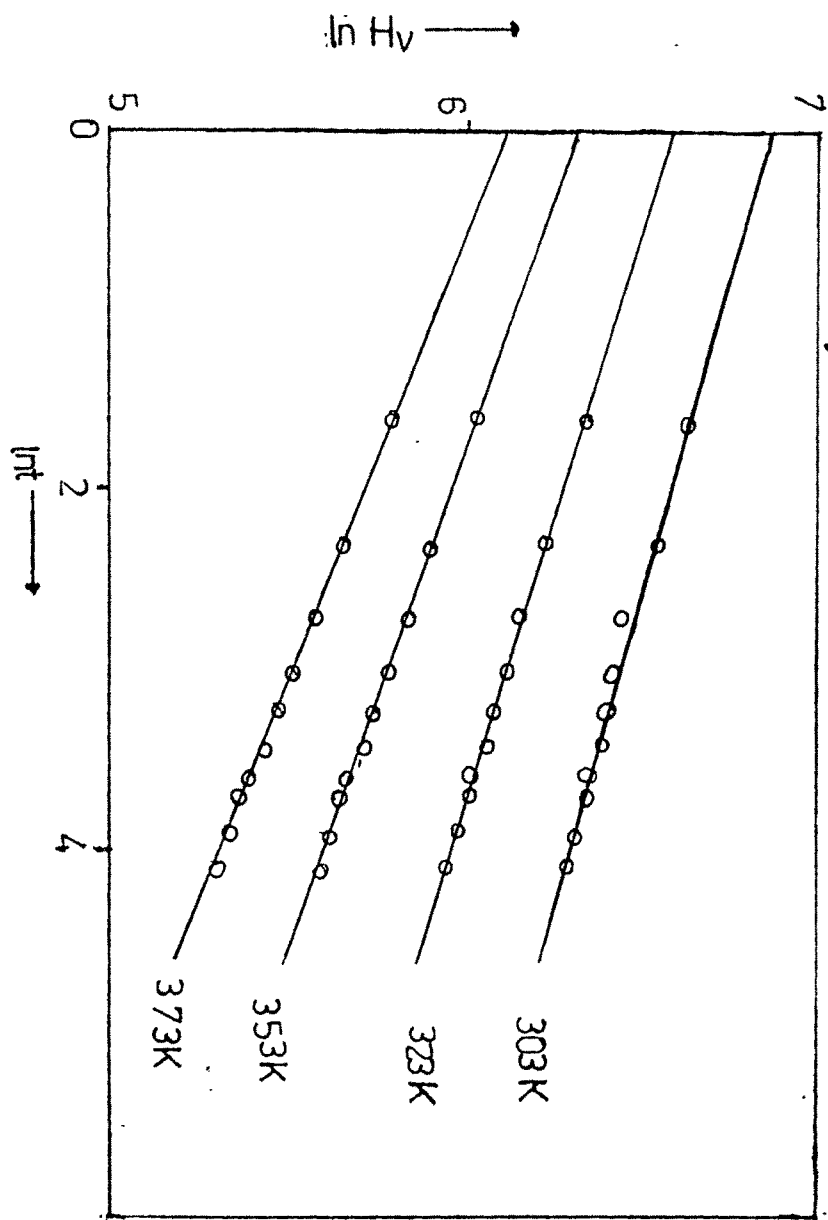


Fig. 13

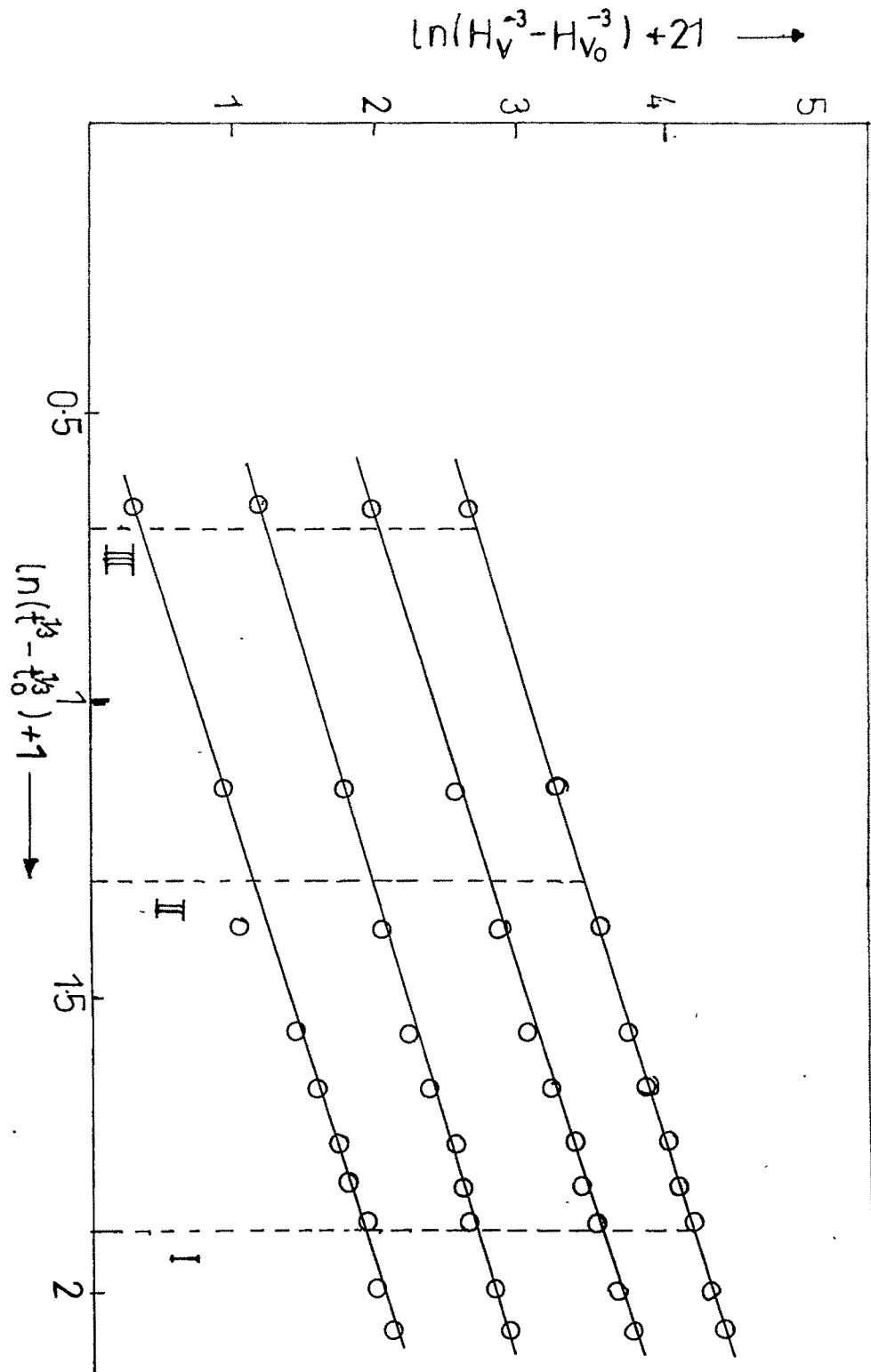


Fig. 14

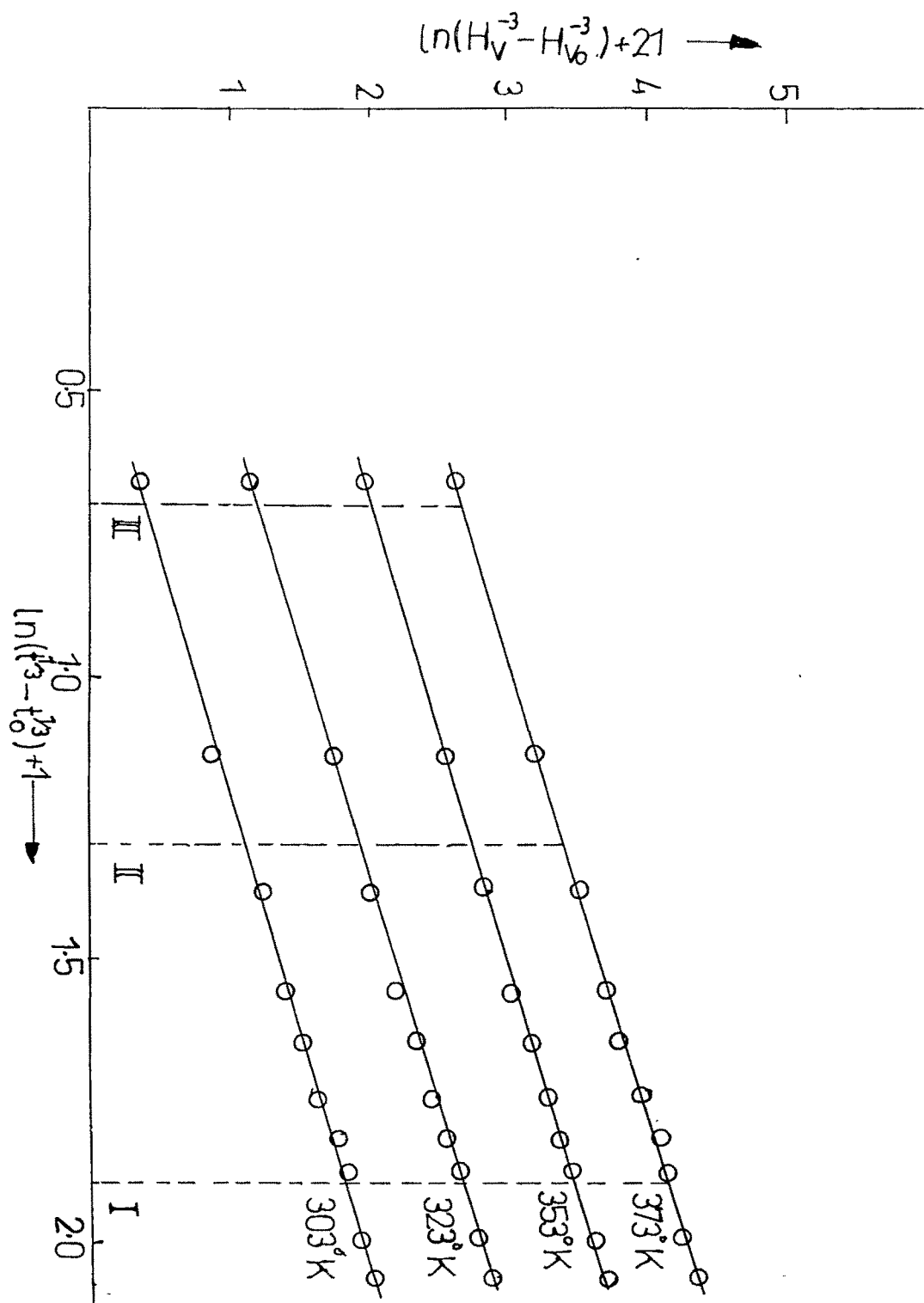


Fig. 15

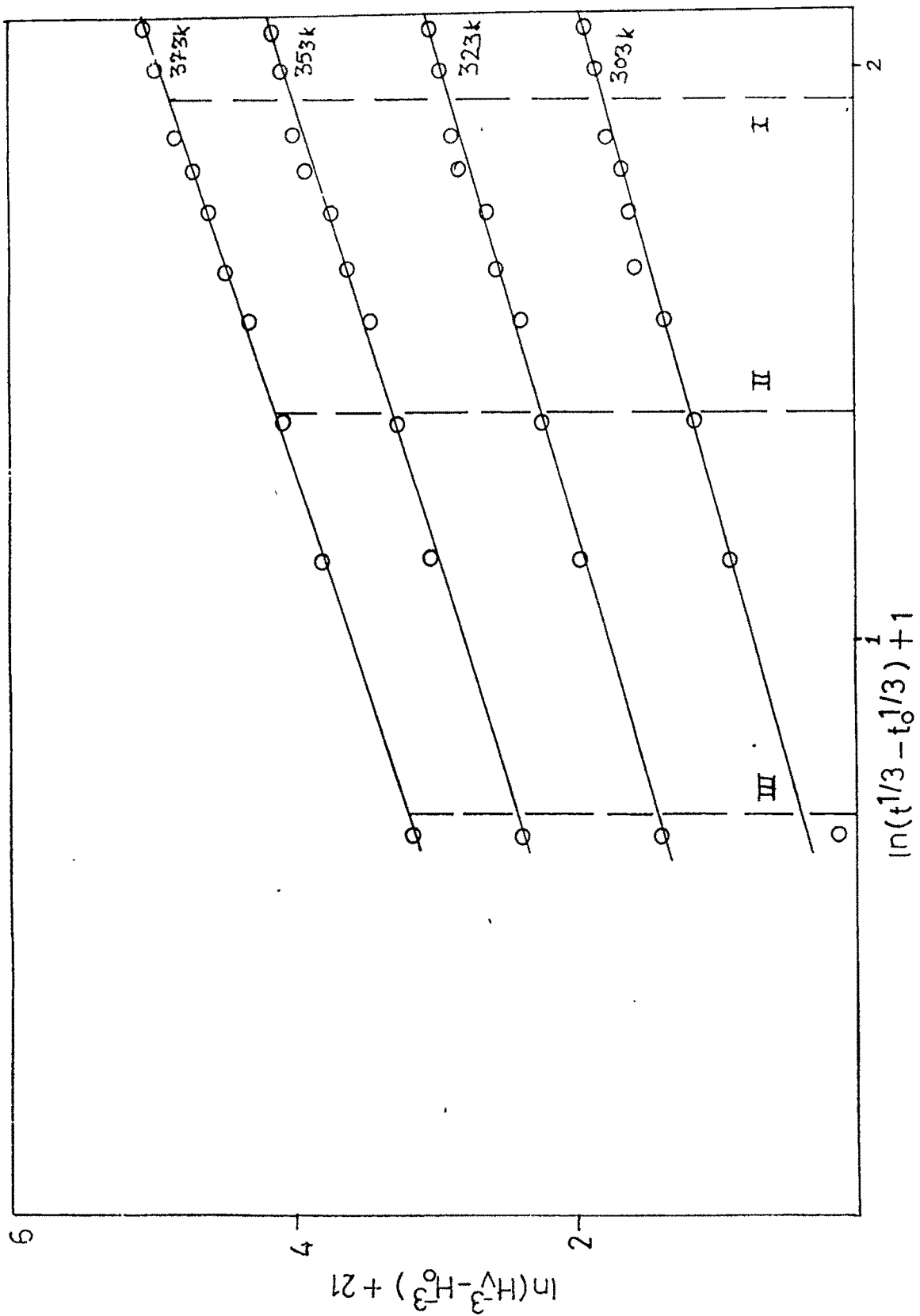


Fig. 16

Under the assumption that Q remains constant with temperature. However, in many cases Q has been found to be different in different temperature ranges. Hence an alternative method (Bhatt and Desai 1982; Jani et al 1995)^[60,61], which does not assume Q to be constant with temperature has been used. From the plots of Figures 14,15 and 16 three sets of $\ln(H^3 - H_0^{-3})$ values at different temperatures were obtained for three different values of $\ln(t^{1/3} - t_0^{1/3})$ indicated by vertical broken lines. These values of $\ln(H^3 - H_0^{-3})$ were plotted against the inverse of corresponding temperature (Figures 17,18 and 19). Again these curves are straight lines with approximately equal slopes according to (2). The slope represents the value of $-Q/3R$. The energy values obtained in the present cases are 23.01, 22.31 and 28.45 Kcal/mole for $Sb_{0.2} Bi_{1.8} Te_3$, $Sn_{0.2} Bi_{1.8} Te_3$ and $Bi_2 Te_{2.8} Se_{0.2}$ crystals. These values are similar to those at low homologous temperature in the cases like Ag, Cu, Ni, Co etc. A dislocation pipe diffusion mechanism may explain this.

Effect of Quenching :

Raising temperature of crystals and quenching them has an effect similar to work hardening. The crystals were raised to various high temperatures in vacuum and were maintained at respective temperatures for about 36 hours. The vacuum sealed ampoule carrying the sample was then quenched by dropping it off the furnace into an ice-bath. The plots of H_v v/s P

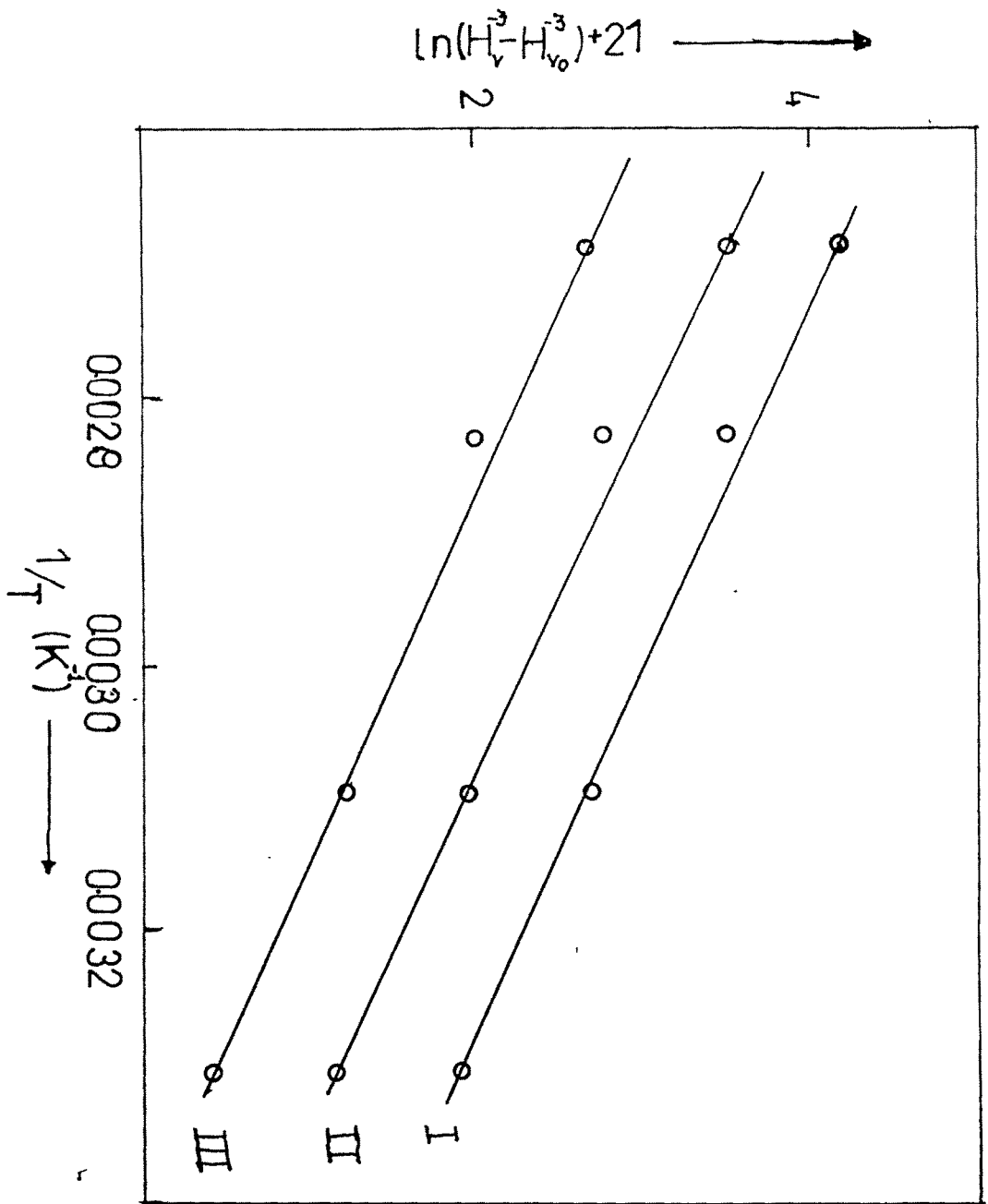


Fig. 17

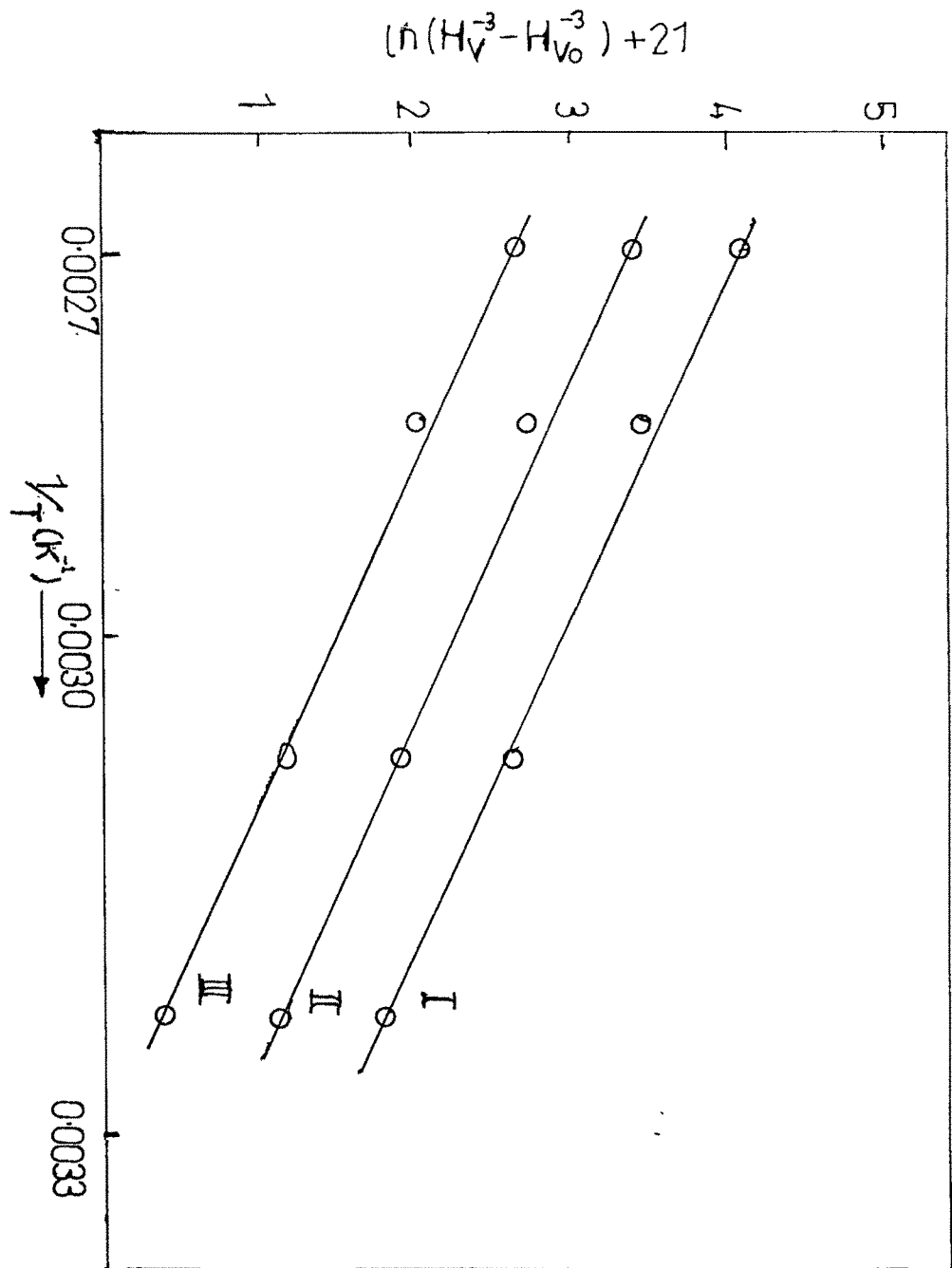


Fig. 18

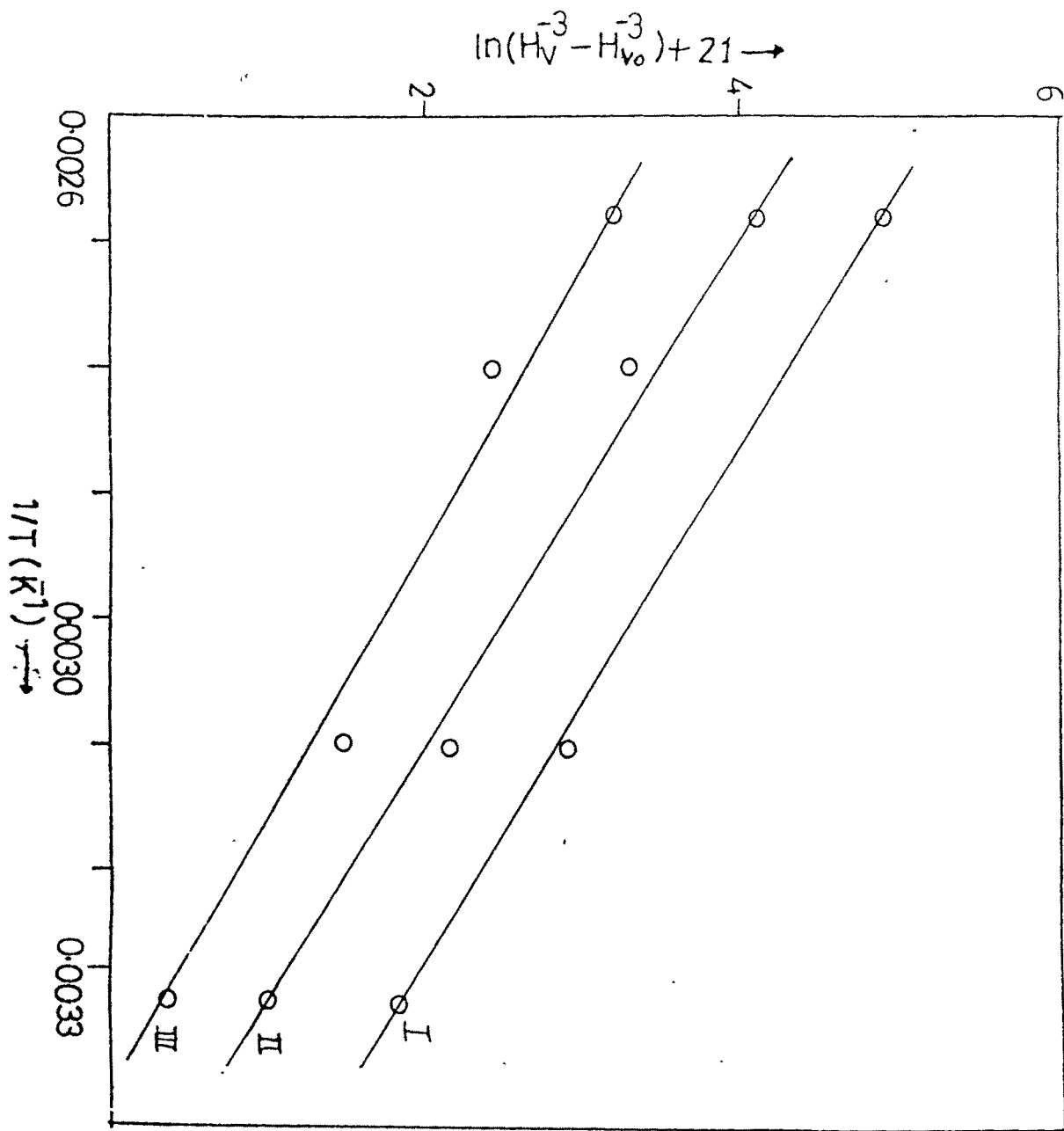


Fig. 19

obtained for various quenching temperatures are shown in Figures 20,21 and 22 for $\text{Sb}_{0.2} \text{Bi}_{1.8} \text{Te}_3$, $\text{Sn}_{0.2} \text{Bi}_{1.8} \text{Te}_3$ and $\text{Bi}_2 \text{Te}_{2.8} \text{Se}_{0.2}$ crystals, respectively. It can be seen in general that the hardness has increased with quenching temperature indicating the quench hardening phenomenon. The dependence of hardness on quenching temperature is known to follow a power law^[15]

$$HT_Q^K = A \quad \text{.....6}$$

Where T_Q = quenching Temperature
A and K = constants
H = hardness

The data obtained in the present study are in agreement with this relation. The plots of $\log H_v$ v/s $\log T_Q$ are shown in Figures-23,24,and 25 for the $\text{Sb}_{0.2} \text{Bi}_{1.8} \text{Te}_3$, $\text{Sn}_{0.2} \text{Bi}_{1.8} \text{Te}_3$ and $\text{Bi}_2 \text{Te}_{2.8} \text{Se}_{0.2}$ crystals, respectively. The lowest T_Q corresponds to room temperature (untreated).

The quench hardening indices, K, obtained from the respective plots are found to be about -0.67, -0.8 and -0.75 for $\text{Sb}_{0.2} \text{Bi}_{1.8} \text{Te}_3$, $\text{Sn}_{0.2} \text{Bi}_{1.8} \text{Te}_3$ and $\text{Bi}_2 \text{Te}_{2.8} \text{Se}_{0.2}$ crystals, respectively.

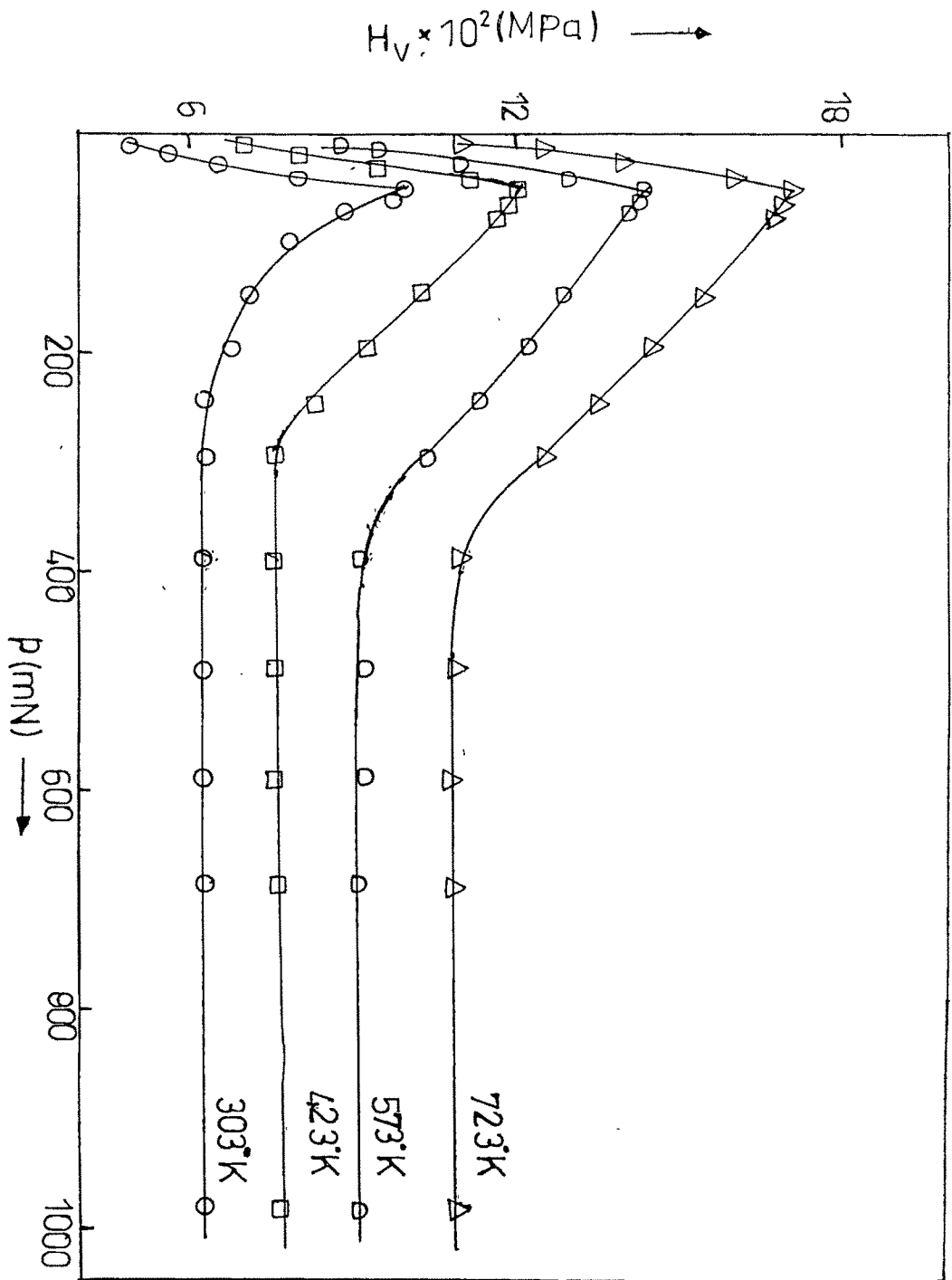


Fig. 20

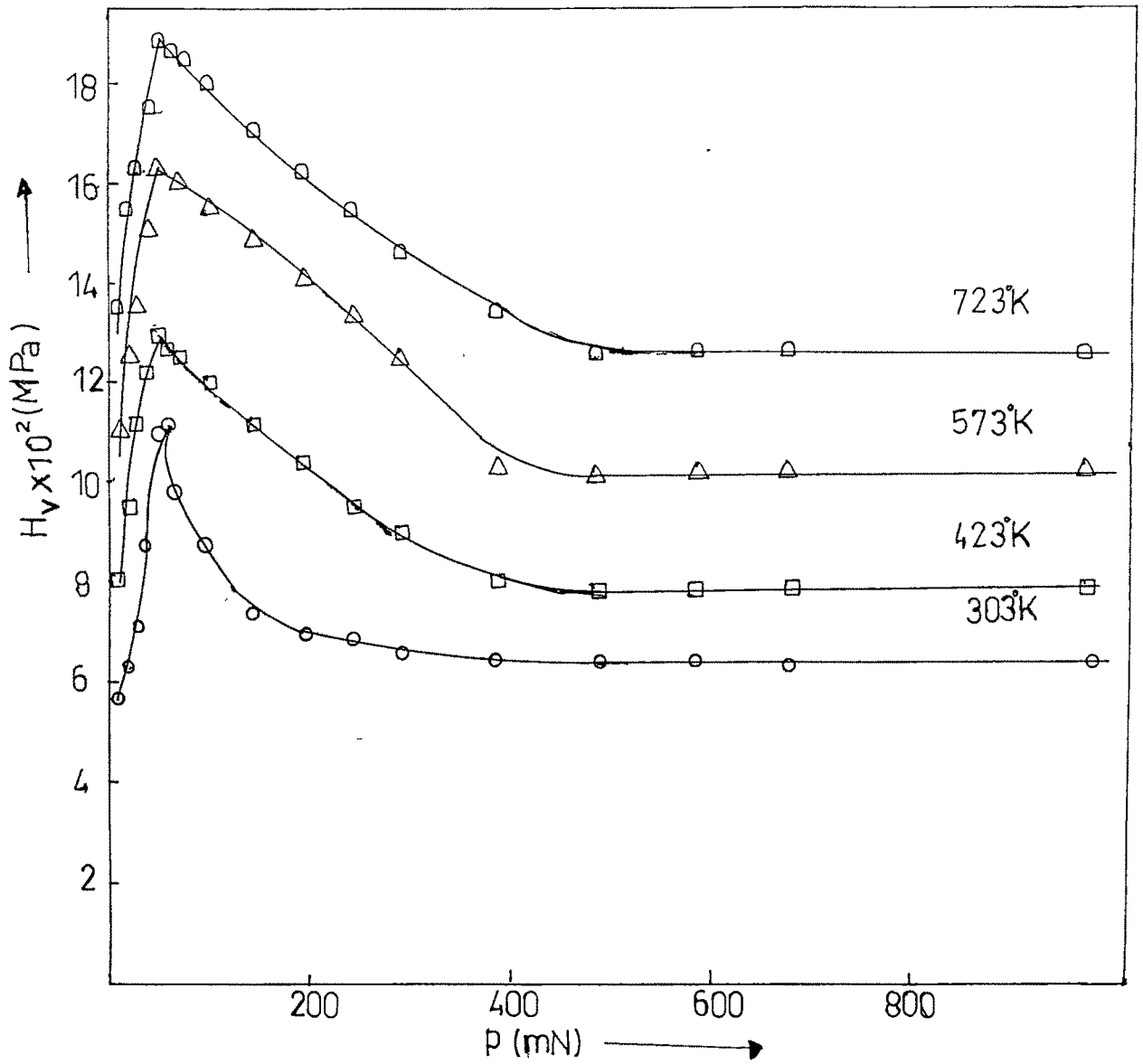


Fig. 21

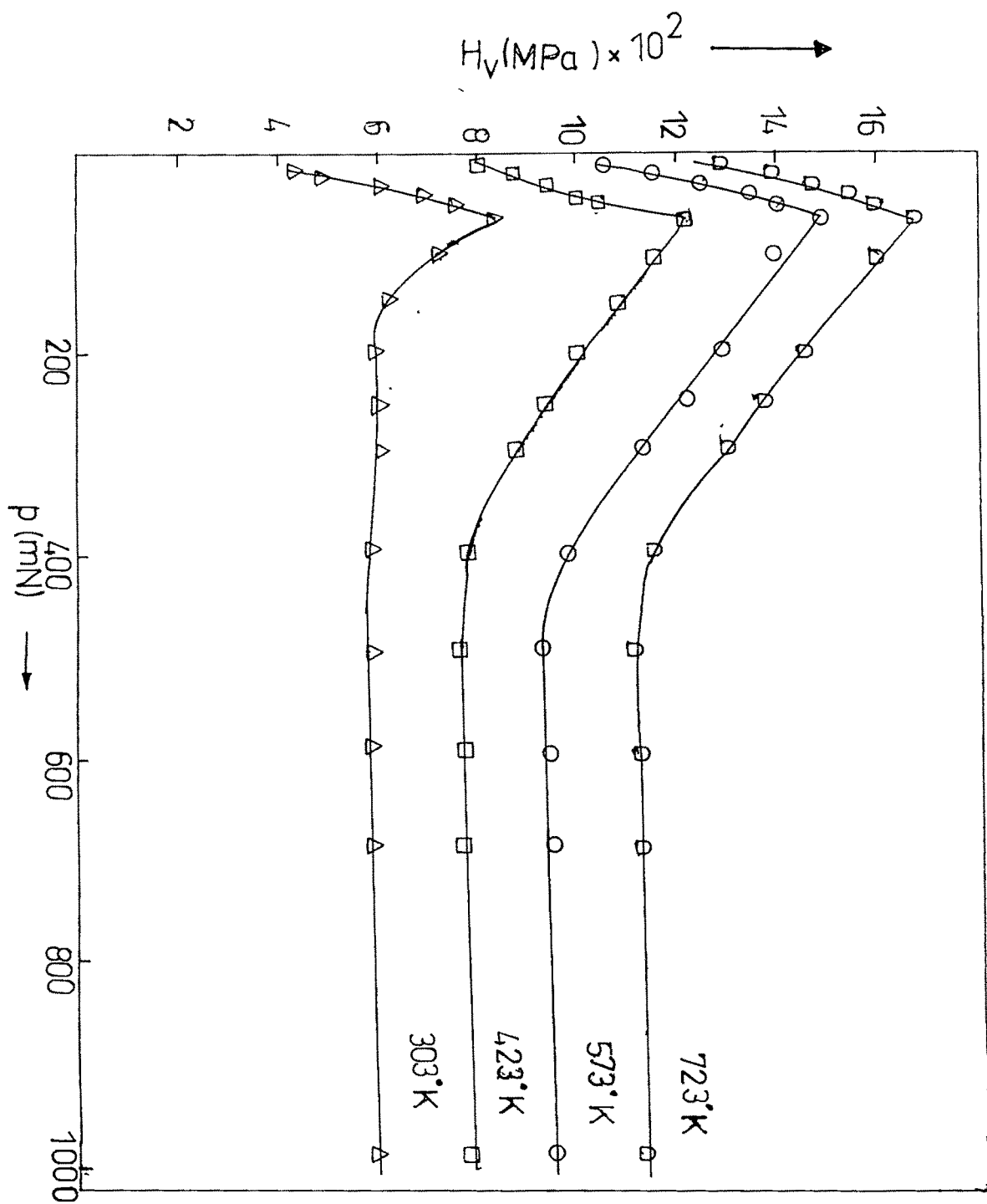


Fig. 22

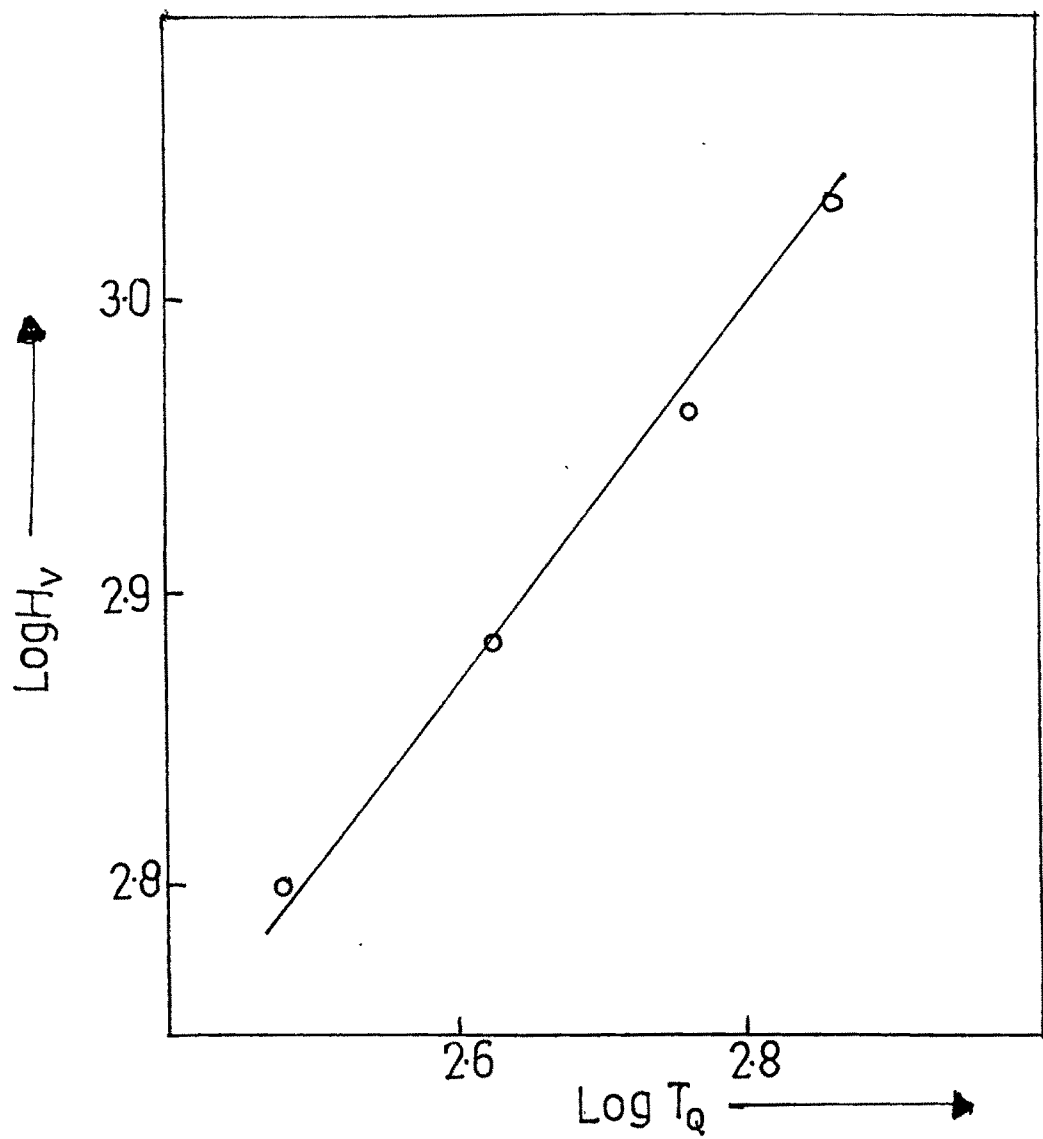


Fig. 23

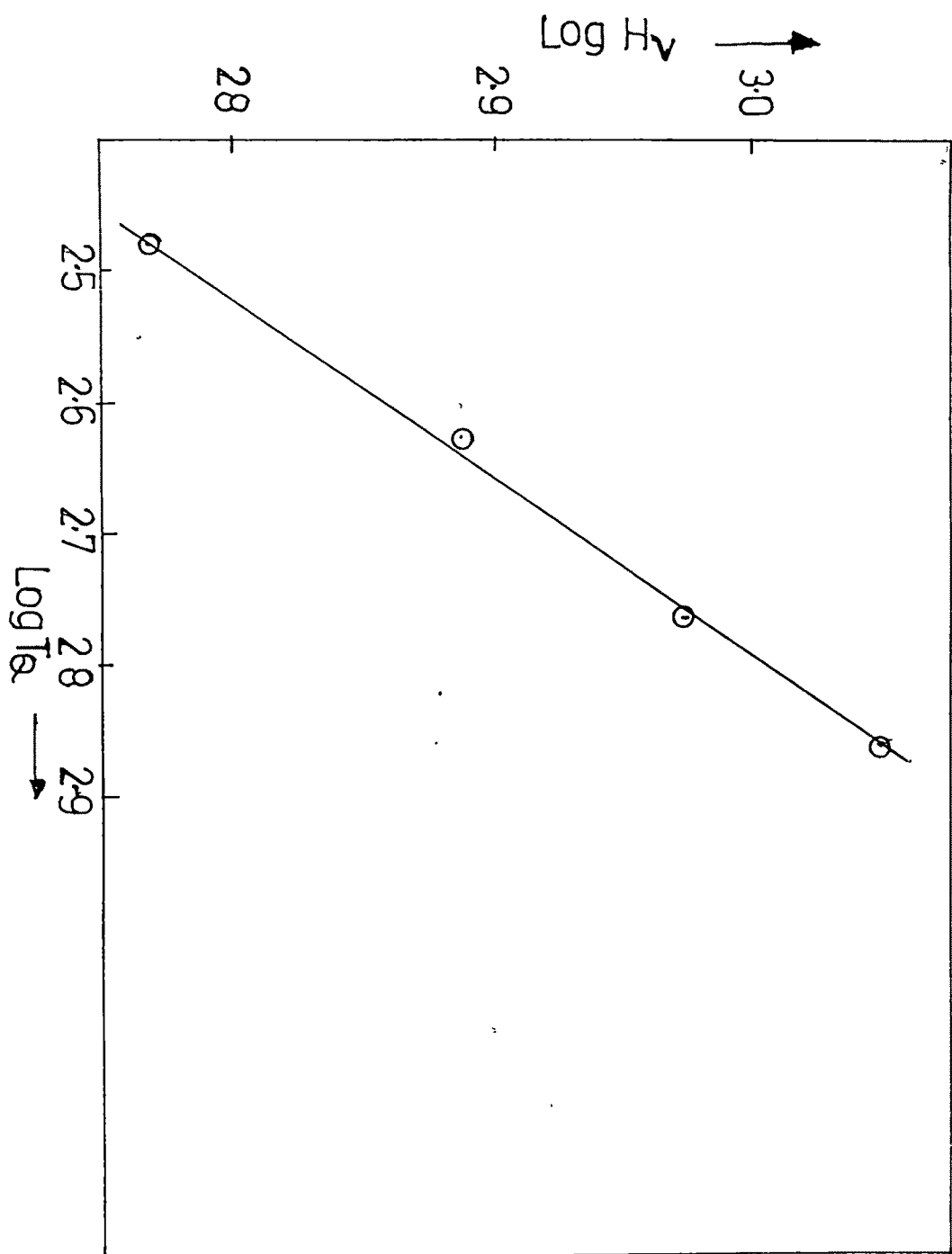


Fig. 24

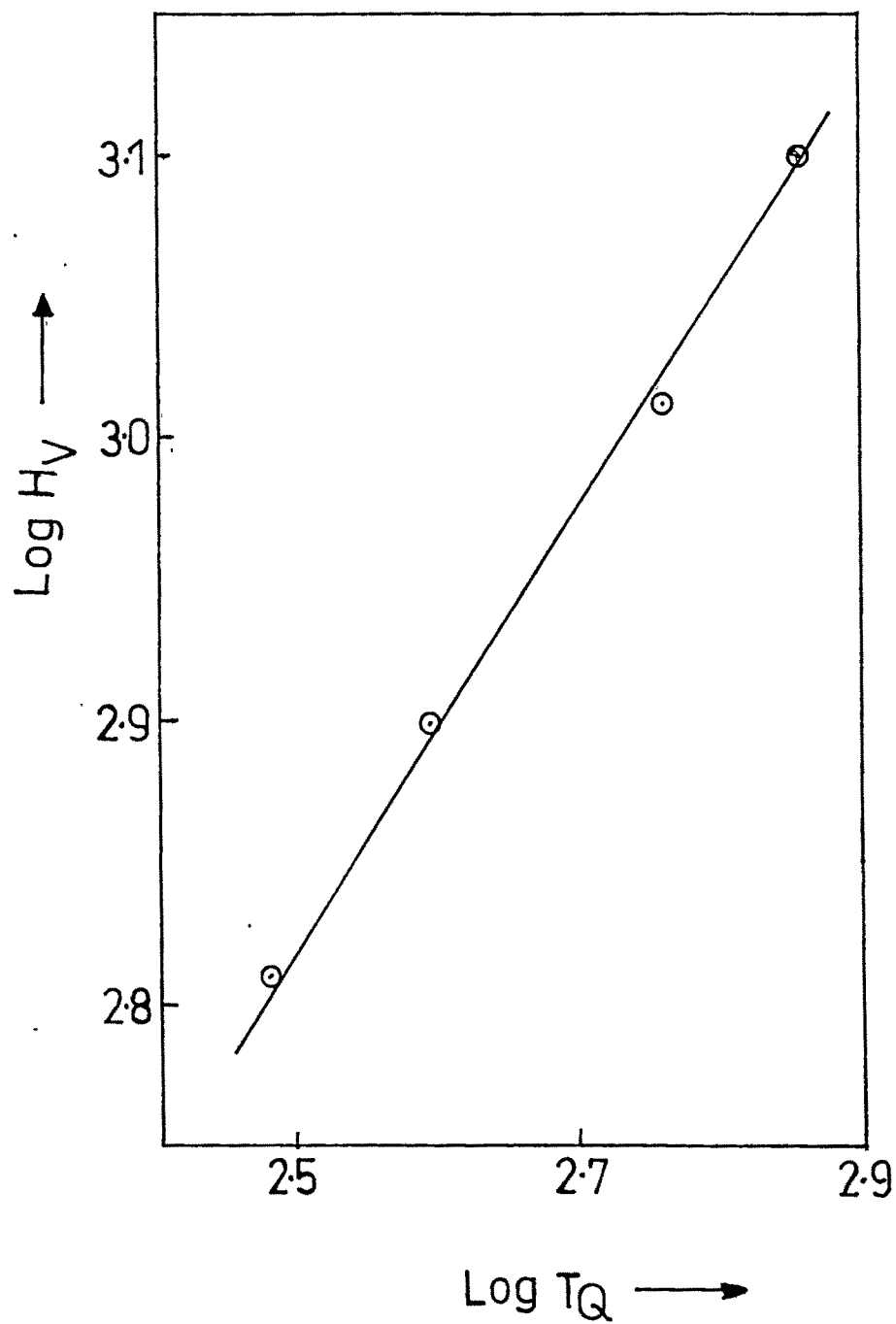


Fig 25

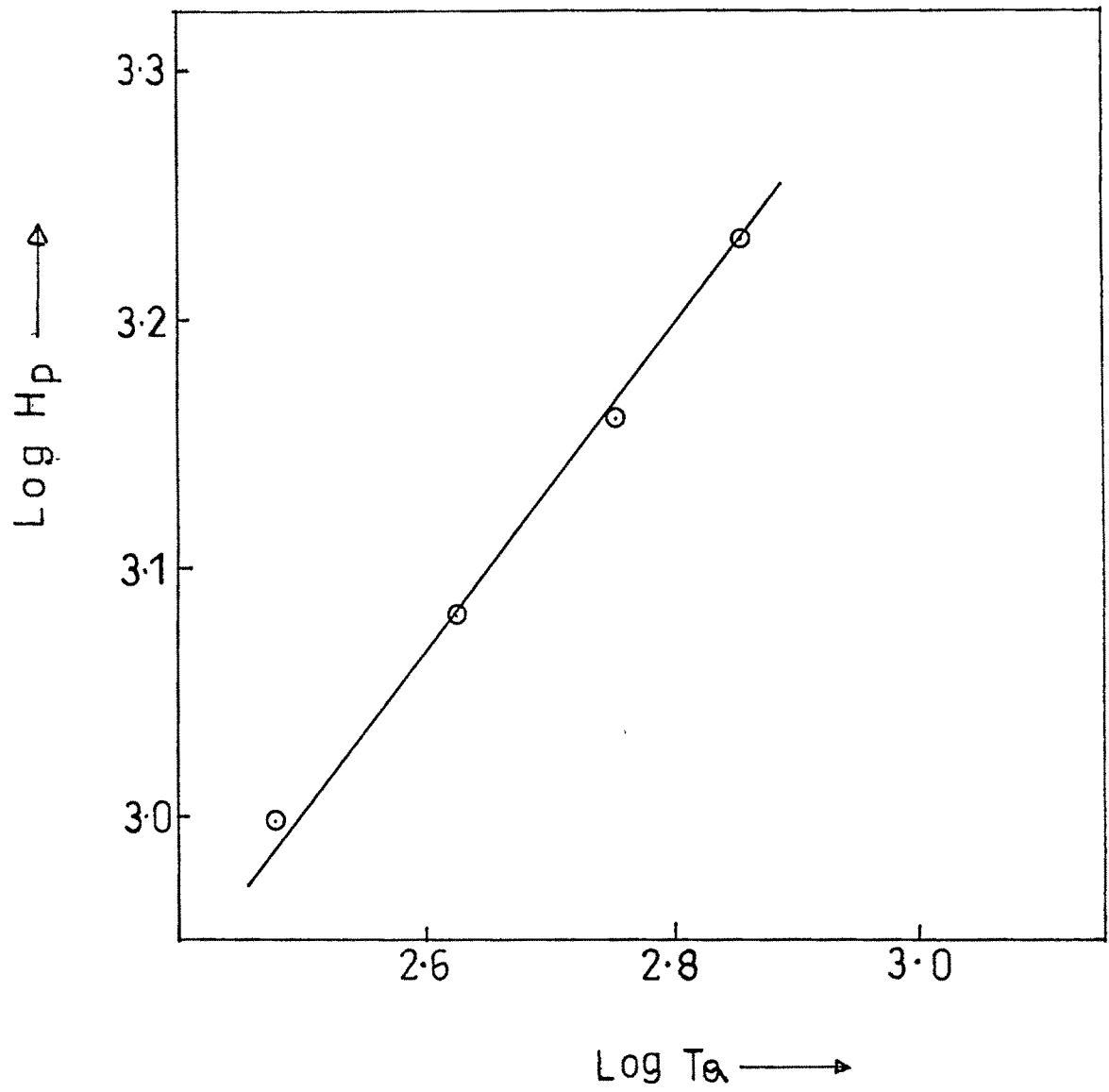


Fig. 26

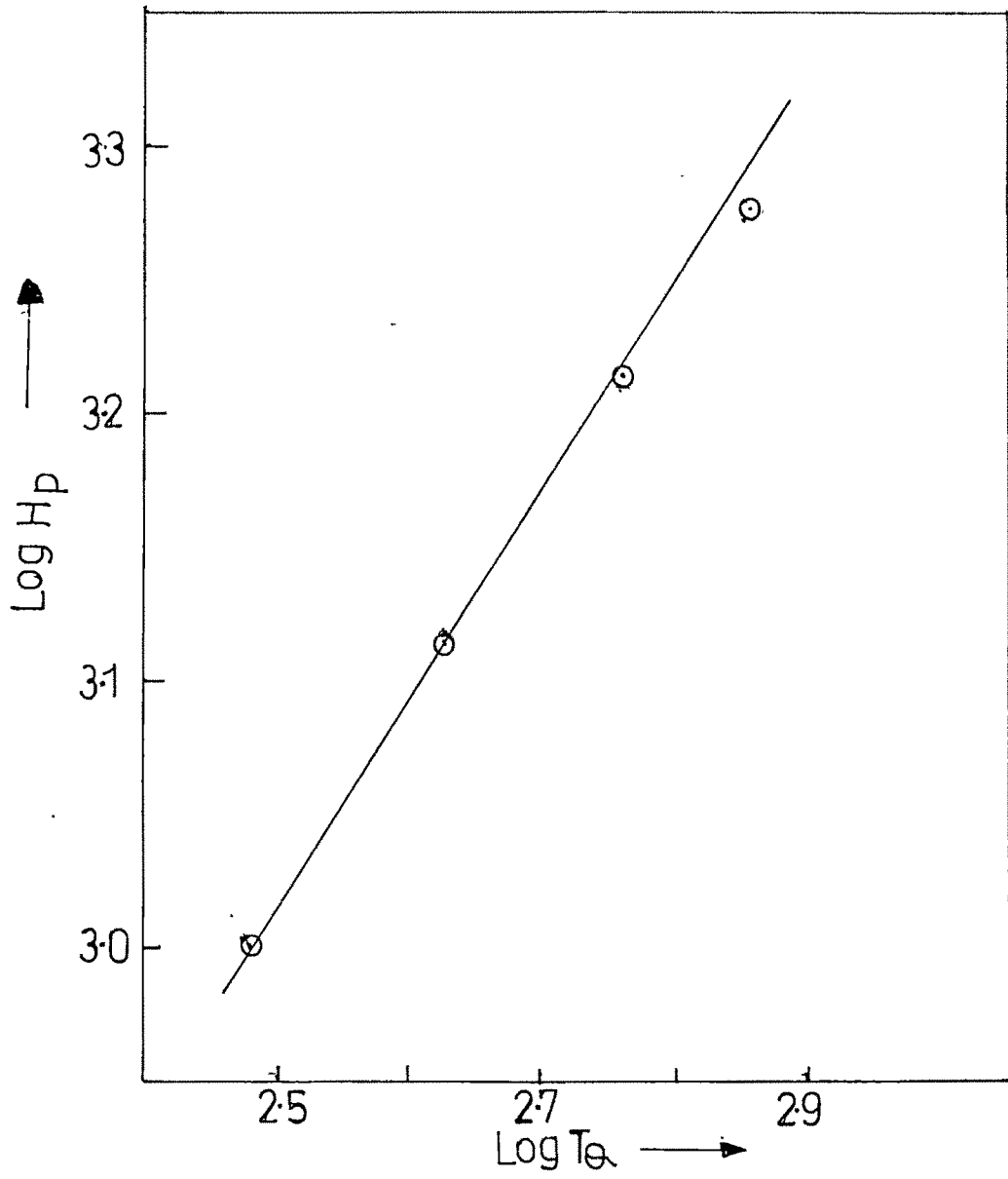


Fig. 27

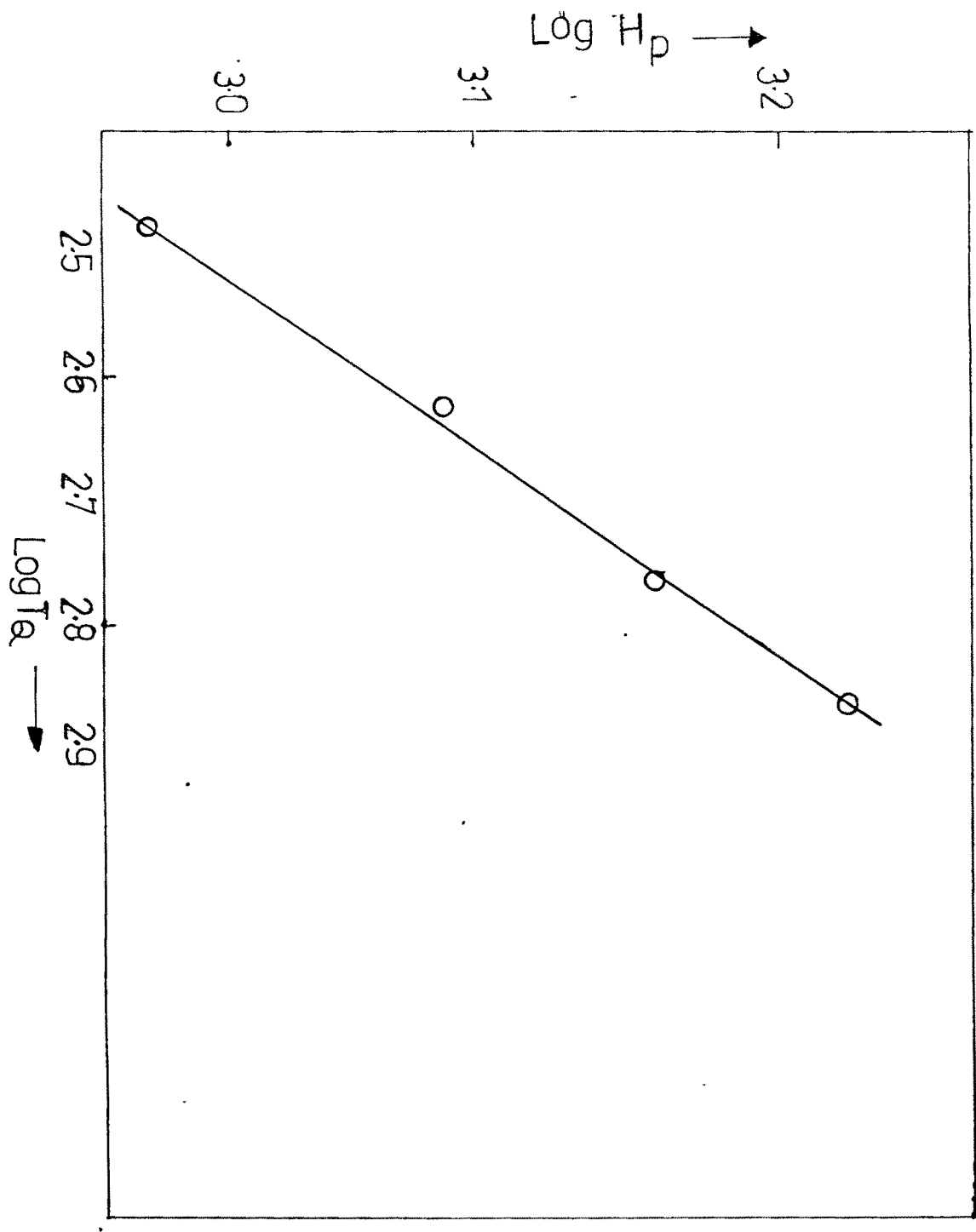


Fig. 28

The general nature of load dependence of hardness of all the three crystals are similar. The effect of quenching on the magnitude of hardness and on the extent of coherent region also follows similar trends in the crystals. The quench-hardening index K being a material constant, plots on the basis of the above equation were obtained by substituting H by H_p , the peak hardness (Figures-26,27 and 28). The slopes of these graphs again yield nearly the same value of K as obtained by the plots in Figures-23,24 and 25. The result highlights the significance of the hardness peaks in defining coherent regions.

Hardness Anisotropy :

In order to study the anisotropy exhibited by the (111) planes of the crystals, the directional hardness was obtained by producing indentations at various azimuthal orientations of the indenter with respect to the surface over a range of 0° to 180° . The reference 0° orientation was set as follows. It was observed while cleaving these crystals that apart from the wavy and irregular cleavage lines there were also some well defined rectilinear cleavage lines

produced. In etching experiments such lines were found to be parallel to the etch pit rosettes obtained in the deformed specimens, These cleavage lines therefore ought to be in crystallographic directions. Hence these directions were chosen as reference directions along which the diagonal of the indentation mark was set to correspond to 0° orientation. The crystal was rotated about the indenter axis in steps of 15° while keeping applied load and loading time constant at 494mN and 20 sec., respectively.

The plots of the measured hardness H_v v/s orientation θ are shown in Figures 29, 30 and 31 for $Sb_{0.2} Bi_{1.8} Te_3$, $Sn_{0.2} Bi_{1.8} Te_3$ and $Bi_2 Te_{2.8} Se_{0.2}$ crystals. It can be seen that the hardness values repeat periodically at 30° intervals. Further, there are distinct maxima and minima which are also periodic. The plots show a periodicity corresponding to a 12 fold symmetry about the loading axis which in the present case, is normal to the cleavage plane (111). This is a result of the 3 fold symmetry of the crystals combined with the 4-fold symmetry of the indenter. It can be seen that there is maximum anisotropy (of about 20%) in the case of the Sn doped crystals. It is known that the resolved shear stress produced by the applied force on the slip systems in a crystal is a function of orientation of the force axis relative to the slip planes and directions. Therefore certain orientations are favourable for the indenter to produce deformation as compared to other orientations. In view of this, the hardness peaks observed above occur at such favourable orientations; whereas the minimum corresponds to the least favourable

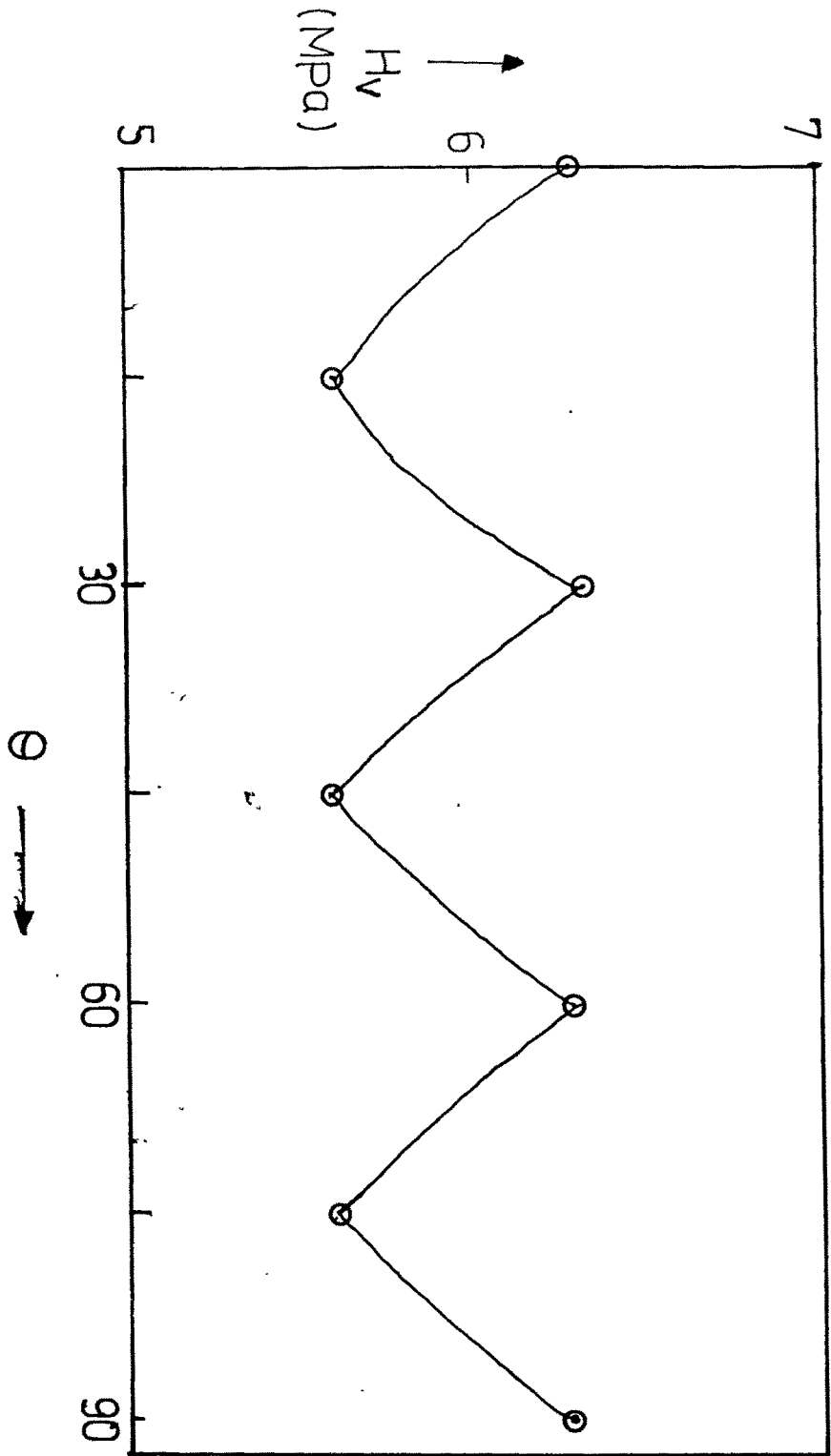


Fig. 29

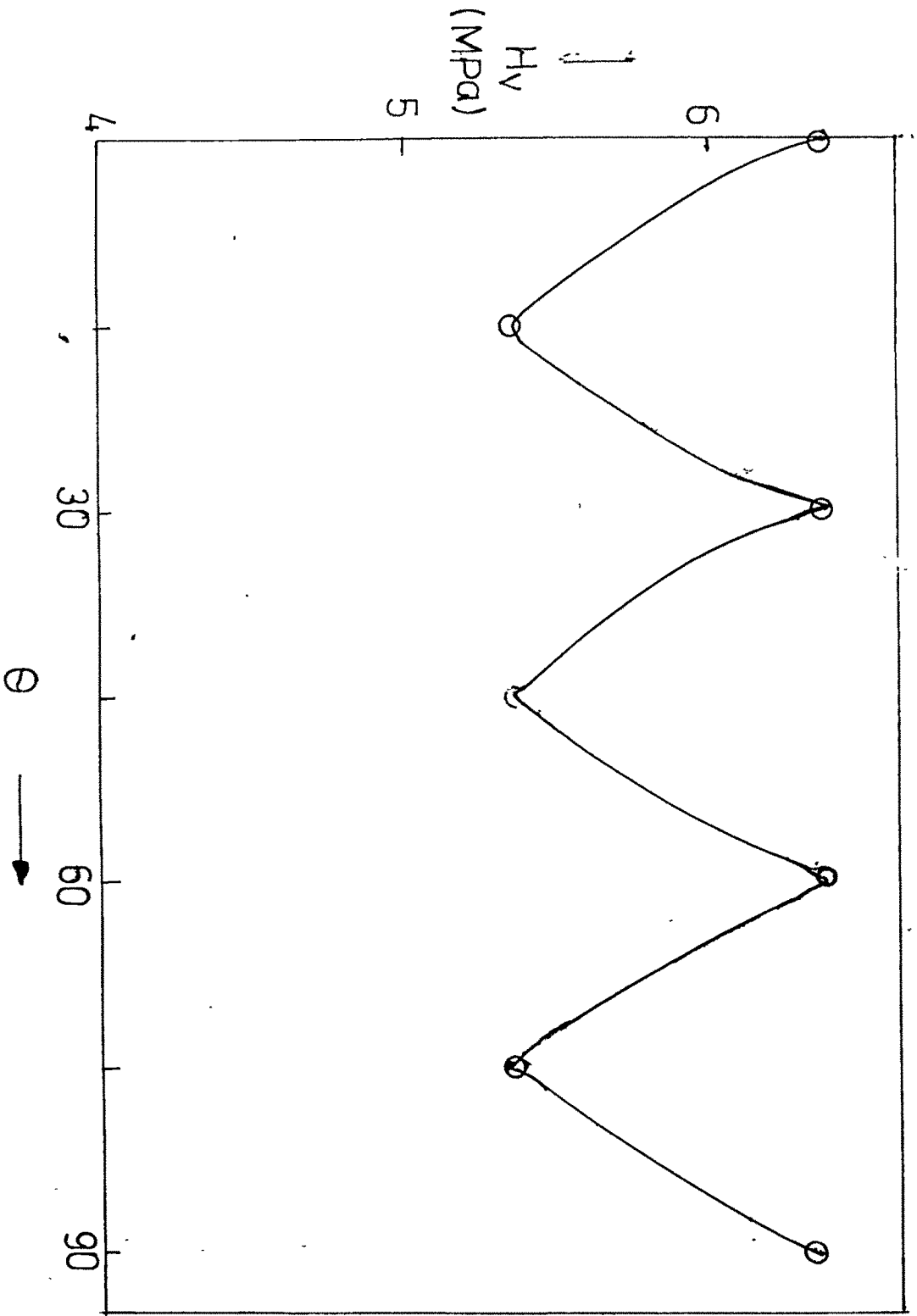


Fig.30

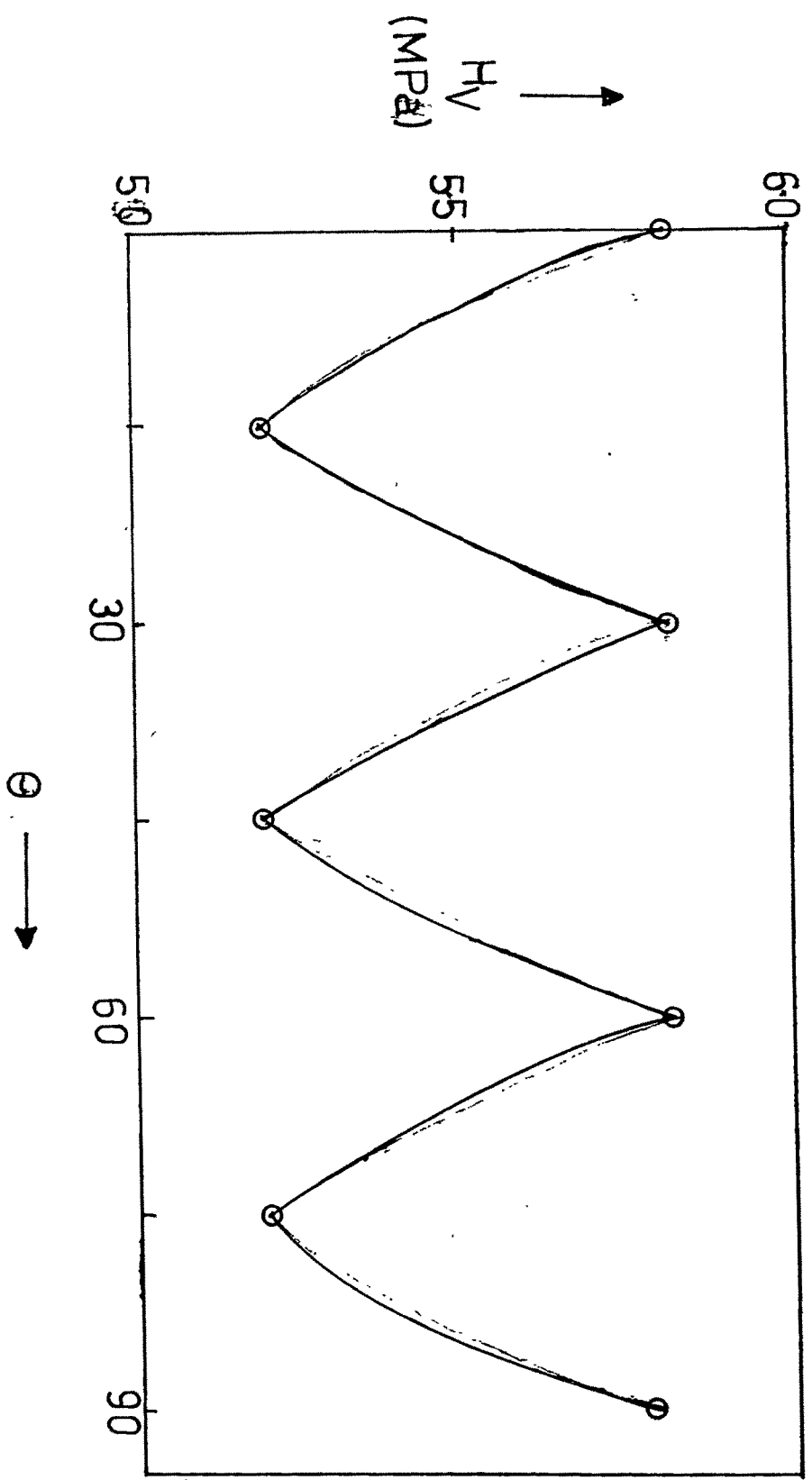


Fig.31

orientations. Maximum to minimum value ratios of hardness are found to be 1.12, 1.54 and 1.11 [$\text{Sb}_{0.2}\text{Bi}_{1.8}\text{Te}_3$, $\text{Sn}_{0.2}\text{Bi}_{1.8}\text{Te}_3$ and $\text{Bi}_2\text{Te}_{2.8}\text{Se}_{0.2}$]. Thus there is practically no anisotropy observed in Vickers hardnesses of $\text{Sb}_{0.2}\text{Bi}_{1.8}\text{Te}_3$ and $\text{Bi}_2\text{Te}_{2.8}\text{Se}_{0.2}$, whereas there is quite significant anisotropy observed in the case of $\text{Sn}_{0.2}\text{Bi}_{1.8}\text{Te}_3$ crystals. The hardness anisotropy coefficients defined as the ratio of the difference between maximum and minimum hardness to the maximum one, are found to be 0.11, 0.10 and 0.16, respectively, for the three crystals.

IV. CONCLUSIONS :

1. The hardness values of $\text{Sb}_{0.2}\text{Bi}_{1.8}\text{Te}_3$, $\text{Sn}_{0.2}\text{Bi}_{1.8}\text{Te}_3$ and $\text{Bi}_2\text{Te}_{2.8}\text{Se}_{0.2}$ single crystals have been obtained to be 630, 642 and 582 MPa, respectively, which are significantly higher than the reported hardness of the pure Bi_2Te_3 crystals.
2. Microhardness is load dependent quantity and the variation is quite prominent in the low load ranges and only for sufficient high applied loads it becomes virtually independent of load.
3. The hardness peaks observed in H_v versus load (P) plots may be explained in terms of deformation induced coherent regions.
4. Due to work hardening, the crystal hardness increases. The Meyer index is not truly constant but may be different in different load ranges.
5. The work hardening capacity of $\text{Sn}_{0.2}\text{Bi}_{1.8}\text{Te}_3$ crystals has been observed to be the highest among the three crystals.
6. The surface anisotropic variations of hardness are observed to be maximum (~20%) in the case of $\text{Sn}_{0.2}\text{Bi}_{1.8}\text{Te}_3$ crystals.
7. The softening parameters of $\text{Sb}_{0.2}\text{Bi}_{1.8}\text{Te}_3$, $\text{Sn}_{0.2}\text{Bi}_{1.8}\text{Te}_3$ and $\text{Bi}_2\text{Te}_{2.8}\text{Se}_{0.2}$ single crystals were found to be 132.40×10^{-4} K, 162.60×10^{-4} K and 84.5×10^{-4} K, respectively.
8. The indentation creep behaviour of the crystals approximates to the relation given by Atkins et al. The creep activation energies in the

temperature range used have been found to be about 23.01, 22.31 and 28.45 Kcal/mole for $\text{Sb}_{0.2} \text{Bi}_{1.8} \text{Te}_3 \text{Sn}_{0.2}$, $\text{Bi}_{1.8} \text{Te}_3$ and $\text{Bi}_2 \text{Te}_{2.8} \text{Se}_{0.2}$ single crystals, respectively.

REFERENCES :

1. Tuckerman, L.B., Mech. Eng., 47 (1925) 53-5.
2. Ashby, N.A., N.Z.Engng., 6 (1951) 33.
3. Meyer, E.Z., Verdeutsch Ing., 52 (1908) 645.
4. Tertsch, H.Z. Krist., 92 (1935) 39-48 and Neus jahrb. Mineral, Monatsh, (1951) 73-87.
5. Mott, B.W., Micro-Ind. Hardness Testing (Butter-Worths Publ.) London, (1956).
6. Gilman, J.J. and Roberts, B.W., J. Appl. Phys., 32 (1961) 1405.
7. Chatterjee, G.P., Ind. J. Phys., 28 (1956) 9-20.
8. Plendl, J.N. and Gielisse, P.J., Phys. Rev., 125 (1962) 828-32.
9. Matkin, D.I. and Caffyn, J.E., Trans. Brit. Ceram. Soc., 62 (1963) 753-61.
10. Westbrook, J.H. and Conrad, H., The Science of Hardness and Its Research Application, American Soc. For metals, Ohio, (1973).
11. Gilman, J.J., The Science of Hardness Testing and Its Research Applications, eds. J.H. Westbrook and H. Conrad (ASM, Ohio), (1973) 51.
12. O'Neill, H., Hardness Measurements of Metals and Alloys, Chapman and Hall Ltd. (London), (1967).
13. Brookes, C.A. and Moxley, B., J. Phys., E8 (1975) 456.
14. Shaw M.C., The science of Hardness Testing and its Research

- Applications, eds. J.H. Westbrook and H. Conrad (ASM, Ohio), (1973).
16. Schmidt E. and Boas W., *Naturwiss*, 20 (1955) 416.
 17. Partridge P.W., *Nature*, 203, (1964) 634-5.
 18. Phael C., *Phil. Mag.*, 10 (1964) 887-91.
 19. Vahldick F.W., *Jap. J. Appl. Phys.*, 5 (1966) 663.
 20. Tolansky S. And Nicholas D.G., *Nature*, 164 (194) and *Phil. Mag.* 43 (1952) 410.
 21. Crocker A.G. and Abell, J.G., *Phil. Mag.*, 33 (1976) 305.
 22. Hess J. and Barrett C.S., *Trans AIME*, 185 (1949) 599.
 23. Flewitt P.E.J., *Phil. Mag.*, 34 (1976) 877.
 24. Van Bueren H.G., *Imperfections in Crystals* (North Holland) (1960).
 25. Cottrell A.H., *Dislocations and Plastic Flow in Crystals* (Oxford Univ.).
 26. Reed-Hill R.E., *Physical Metallurgy Principles* (Van Nostrand) (1964).
 27. Barrett, C.S., *Dislocations and Mechanical Properties of Crystals* Eds., J.C.Fisher et al. (Wiley) (1965).
 28. Lawn, B.R., and Wilshaw, T.R., *Fracture of Brittle Solids* (Cambridge Univ.) (1975).
 29. Taplin, D.M.R., (Ed) *Rep. 4th Int. Conf. On Fracture*, Waterloo (1977).
 30. Boyarskaya Yu.S., *Cryst. Res. and Tech.* (Germany), 16 (1981) 441.
 31. Shah B.S. and Mathai M.B., *Current Sci.* (India), 38 (1969) 4780.

32. Knoop, F., Tech. Blatter, 27 (1973) 472.
33. Bernhardt E.O., Z. Metalk, 33 (1941) 135.
34. Campbell R.F., Honderson O., and Donleavy M.r., Trans. A..S.M. 40 (1948) 954.
35. Mott, W.B., Ford S.D. and Jones I.R.W., AERE, Harwell Report IR, 1 (1952) 017.
36. Taylor E.W., J.Instr. Metals, 74 (1948) 493.
37. Bergsman E.B., Met. Progr., 54 (1948) 183.
38. Hanemann H., Z. Metallak, 33 (1941) 124.
39. Onitsch E.M., Mikroskopie, 2 (1947) 131-4.
40. Grodzinski P., Ind. Diamond Rev., 12 (1952) 209, 235.
41. Walls M.G., Chaudhri, M.M. and Tang T.B., J. Phys. D., Appl. Phys. (UK), 23, (3), (1992) 500-7.
42. Onitsch, E.M., Schweiz Arch, Angew Wiss, 19 (1953) 320.
43. Buckle H., Rev. Mettal, 48(1951) 957.
44. Bochvar A.A. and Zhadaeva O.S., Bull. Acad Sci., URSS, 3 (1947) 341.
45. Onitsch E.M. Mikroskopie, 2 (1947) 131.
46. Buckle H., Rev. Metall, 48 (1951) 957.
47. Br. ^A _v ~~q~~unovic, The Sci. Of Hardness Testing and its Research Applications, eds., westbrook and Conrad H., (ASM, Ohio), (1973)4.

48. Chen and Hendrickson, The Sci. of Hardness Testing and its Applications, Eds. By Westbrook and Conrad H., (ASM, Ohio), (1973)4.
49. Ito, K., Sci Papers Sandai, Tohoku Univ. Ser.1, 12 (1923) 137.
50. Shishokin V.P., Z. Anorg. Chem., 189 (1930) 263.
51. Hargreaves F., J. Inst. Metals, 39 (1928) 301.
52. Mott, N.F., Phil. Mag., 44 (1953) 742.
53. Atkins A.G., Silverio A. and Tabor D., J. Inst. Metals, 94 (1966) 369.
54. Shah, R.T., Ph.D. Thesis, M.S. Univ. of Baroda (1976).
55. Desai, C.F., Ph.D. Thesis, M.S.Univ. of Baroda (1980).
56. Shah, A.J., Ph.D. Thesis, M.S.Univ. of Baroda (1984).
57. Shah, R.C., Ph.D. Thesis, M.S.Univ. of Baroda (1984).
58. Jani, T.M., Ph.D. Thesis, M.S.Univ. of Baroda (1995).
59. Vyas, S.M., Ph.D. Thesis, M.S.Univ. of Baroda (1998).
60. Bhatt, V.P. and Desai, C.F., (1982) Bull. Mater. Sci. 4 23.
61. Jani, T.M., Pandya G.R. and Desai C.F., (1995) Cryst. Res. Technol. 30 K17.